Materials Advances

ROYAL SOCIETY OF CHEMISTRY

REVIEW

View Article Online
View Journal | View Issue

Cite this: *Mater. Adv.*, 2020, **1**, 2163

Carbon nanofiber-based three-dimensional nanomaterials for energy and environmental applications

Xinxiao Zhou,[a] Bin Liu,[a] Yun Chen,[a] Lei Guo*[b] and Gang Wei *[a]

Carbon nanofibers (CNFs) not only retain a similar one-dimensional nanostructure, similar special properties, and similar multi-functionality to carbon nanotubes, but they also exhibit a few advantages, like easier production, lower cost, lower crystallinity, and more defects. Therefore, CNF-based nanomaterials have been widely used for applications relating to energy conversion/storage, catalysis, sensors, adsorption/separation, and biomedical engineering. Due to their high specific surface area, interconnected porous structure, light weight, and high mechanical strength, CNF-based three-dimensional (3D) nanomaterials have attracted more and more attention in many fields, especially in energy production/storage and environmental science. In this work, we demonstrate the development of CNF-based 3D nanomaterials for applications relating to energy and environmental science. To achieve this aim, typical design strategies for the production of CNF-based 3D nanomaterials, including electrospinning, chemical vapor deposition, templated synthesis, hydrothermal synthesis, and other combined techniques are introduced and summarized, and then cases involving fabricated CNF 3D nanomaterials for supercapacitors, fuel cells, electrochemical batteries, water purification, air cleaning, and microwave/radiation adsorption are presented and discussed. This study will be helpful for readers to understand the production of CNFs, and the subsequent design and fabrication of functional CNF-based 3D nanostructures and nanomaterials; meanwhile it will be valuable for promoting the advanced applications of CNF-based nanomaterials in different fields.

Received 9th July 2020,
Accepted 4th August 2020

DOI: 10.1039/d0ma00492h

rsc.li/materials-advances

1. Introduction

The carbon element is abundant in nature and closely related to human life, and it can be used as a single element to form substances with great differences in properties, such as zero-dimensional (OD) carbon dots (CDs) and fullerene, one-dimensional (1D) carbon nanofibers (CNFs) and carbon nanotubes (CNTs), as well as two-dimensional (2D) graphene. A lot of studies have been performed to explore the unique properties and applications of various carbon nanomaterials. For instance, applications of CDs, CNFs, CNTs, and graphene have been explored in the fields of optoelectronics, energy storage, catalysis, bioimaging, and environmental science due to their excellent fluorescent, thermal, mechanical, and conductive properties.[1–4]

CNF is one of the important carbon nanomaterials that have been used widely, which has similar structure and properties to CNTs, but it has easier production, low cost, and improved functions.[5,6] CNFs reveal smooth, porous, hollow, helical, and stacked-cup structures, and they have good thermal conductivity, electric conductivity, and high specific surface area, which make them excellent nanoscale building blocks for the synthesis of CNF-based functional nanomaterials.[7] In order to produce CNFs, several methods, such as electrospinning, chemical vapor deposition (CVD), and templated synthesis, have been widely utilized. For instance, after the electrospun production of polymer nanofibers (PNFs), CNFs could be easily produced *via* carbonization at high temperature.[8,9] The CVD synthesis of CNFs is based on the 1D growth of carbon on substrates through the mediation of special catalysts.[10,11] In addition, 1D natural polymers, such as cellulose, chitin, lignin, and chitosan NFs, provide the possibility of creating CNFs by direct carbonization.[12–14]

With the development of both synthesis and application techniques of CNFs, three-dimensional (3D) CNF-based nanomaterials have attracted a great deal of attention, which is ascribed to their unique properties and functions, like high specific surface area, interconnected porous structure, light weight, and high mechanical strength.[15–17] 3D CNF-based nanomaterials could be synthesized by several techniques, including

[a] *Research Center for High-Value Utilization of Waste Biomass, College of Life Science, Qingdao University, 266071 Qingdao, P. R. China. E-mail: weigroup@qdu.edu.cn, wei@uni-bremen.de*
[b] *College of Life Science, Qingdao University, 266071 Qingdao, P. R. China. E-mail: xianger001@163.com*

electrospinning deposition, CVD, templated synthesis, and hydrothermal synthesis. In some cases, the formation of 3D CNF nanomaterials involves complex processes that include two or three of the techniques introduced above. Compared with 0D, 1D and 2D carbon materials, the advantages of 3D CNF nanomaterials in structure and function expand their applications in many fields.[18,19]

Previously, many reviews have been contributed to this important research field to present the development of synthesis and applications of CNF-based nanomaterials.[20–23] For example, Zhang *et al.* summarized the preparation of electrospun polyacrylonitrile (PAN)-based CNFs for energy conversion/storage, catalysis, sensors, adsorption/separation, and biomedical applications,[20] Feng *et al.* reviewed the synthesis, properties, and applications of CNFs and their composites,[21] and Kim *et al.* presented advances in electrospun CNFs in applications to electrochemical energy storage.[23] All these works provide important information on how to apply the produced CNFs and CNF-based composites for various applications; however, there has been only limited content on the fabrication of 3D CNF-based nanomaterials. Considering the significance of 3D CNF nanomaterials in the fields of energy and environmental science, it is necessary for us to contribute a review article to present the fabrication strategies of 3D CNF nanomaterials, as well as their energy and environmental applications. In the first part, the importance of CNFs and CNF-based nanomaterials is introduced briefly and in the second part, several typical techniques for the fabrication of 3D CNF-based nanomaterials are introduced and discussed. Then, recent advances in 3D CNF nanomaterials in energy and environmental applications are presented in Sections 3 and 4, respectively. Finally, we summarize the achievements and challenges, and comment on the potential research aspects for CNFs.

2. Fabrication of 3D CNF-based nanomaterials

In this part, the main methods for the fabrication of CNF-based 3D nanomaterials are presented and discussed.

2.1. Electrospinning synthesis

Electrospinning is a facile and effective way to create PNFs through spinning polymer precursors into a nanofibrous structure on a collector. During the spinning process, a high voltage is applied between the spinning nozzle and the special collector. Through the interaction of surface force and electrostatic force, the polymer solution at the tip of the spinning nozzle forms a Taylor cone, and finally sprays onto the collector with the accumulation of voltage.[24] During the spraying process, the polymer is stretched and refined into continuous NFs. Finally, NFs are deposited onto a suitable collector substrate to prepare NF mats. After the preparation of PNFs, subsequent post-treatments such as carbonization or calcination are usually needed for the fabrication of CNFs.[25–27]

Electrospinning is a facile technique to fabricate 3D PNF-based scaffolds.[28] In the process of electrospinning, the thickness of the electrospun nanofibrous scaffolds is mainly proportional to the spinning time. Hence, the easiest way to form a 3D structure is to extend the collection time to increase the film thickness. The longer the spinning time, the thicker the material deposited. In addition, the electric field shielding and debilitating effect place a limit on the thickness of the deposited PNFs. However, with the continuous spinning process, it is possible to achieve a certain thickness of the fabricated nanofibrous film in order to achieve a 3D structure of NFs.[29] Meanwhile, the thickness of the electrospun 3D nanofibrous structures could be slightly improved by changing the spinning conditions, such as adjusting the concentration of polymer precursor and the spinning voltage. By alternating spinning in this way, the total thickness of the multilayer PNFs can be increased.

Besides the direct electrospinning fabrication of 3D PNFs structure, the post-treatment of electrospun 1D PNFs and 2D membranes is another way of preparing a 3D PNF structure. Through physical methods, such as folding, expanding, and curling, the structure of 1D PNFs and 2D membranes could be changed to form a stable 3D PNF scaffold. For example, Wang *et al.* improved the performance of a filtration membrane by simply stacking multiple layers of electrospun NFs into a 3D structure.[30] Leung *et al.* changed the glass temperature of the fibers by pressurizing carbon dioxide, which then sintered the fibers together to form a 3D scaffold.[31] In another study, Xu *et al.* spontaneously condensed polycaprolactone (PCL) into a 3D structure by thermal induction.[32]

After the formation of 3D PNF scaffolds by electrospinning, it is possible to fabricate further 3D CNF nanostructures through some post-treatment methods such as the calcination and carbonization of as-produced PNFs.[33,34] For instance, in a typical case Zhang and co-workers demonstrated the fabrication of 3D porous CNFs network with high doping of N and B through an electrospinning and subsequent calcination process, as shown in Fig. 1a.[35] First, a methanol solution containing polyvinylpyrrolidone (PVP) and ammonia borane (AB) was electrospun onto a copper foil to form a 3D PVP–AB NF film, which was then annealed at 850 °C under an N_2 atmosphere for 3 h to form CNFs. The created PVP–AB NFs had a uniform diameter of about 250 nm and the formed 3D CNF film exhibited multiple layers with a thickness of 180 μm (Fig. 1b). After carbonization, the formed N/B-doped CNFs revealed a porous structure and rough surface, as indicated in Fig. 1c and d. In this synthesis process, PVP and AB were chosen for a few reasons. For instance, the good dispersity of PVP with AB promotes the electrospun production of PNFs with a smooth surface and a uniform diameter, PVP provided a good C resource for the formation of CNFs after carbonization, and AB assisted the heteroatom N- and B-doping of C-based materials. Therefore, the selection of PVP and AB with an optimal mass ratio endowed the formation of CNFs with improved electronic, physicochemical, optical, and structural properties. In addition, porous CNFs were synthesized for energy storage applications as the porous C-materials could shorten the transport length of Li^+ ions

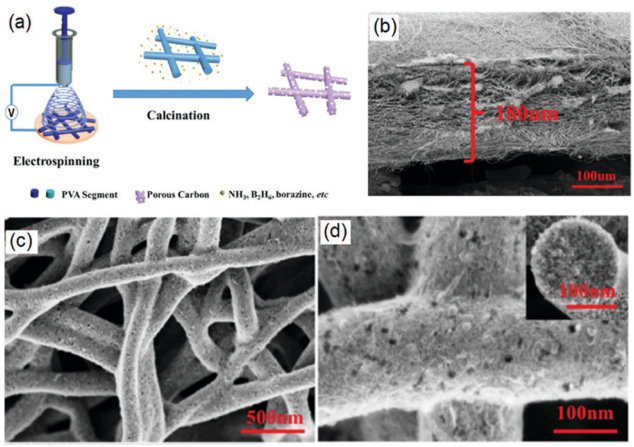

Fig. 1 The electrospinning-based fabrication of 3D CNF-based nanomaterials: (a) fabrication process of a PVA mat and carbonization to a 3D CNF mat, (b) the 3D structure of a PVA mat, and (c and d) SEM images of a CNF mat at different magnifications. Reprinted images with permission from ref. 35. Copyright 2016, Elsevier BV.

and offer a large specific interface for the charge-transfer reaction, resulting in high Li^+ capability and excellent cycling stability. Therefore, the created 3D porous N- and B-doped CNF network exhibited a high specific surface area, good electrical conductivity, and high catalysis properties for energy storage applications.

Through this combined electrospinning and high-temperature treatment process, a lot of 3D CNF structures have been fabricated for various applications. For instance, Cheng *et al.* demonstrated the synthesis of 3D CNFs by electrospinning a mixture of montmorillonite and PAN, carbonizing the electrospun PNFs, and subsequent acid etching.[36] Tiwari and co-workers presented the synthesis of a highly porous 3D CNF network anchored with Co NPs *via* combined electrospinning and subsequent post-treatments.[37] Therefore, the electrospinning production of 3D PNFs is the first step and the next step of calcination/carbonization is necessary for the fabrication of 3D CNFs by using the nanofibrous structure of PNFs and the numerous carbon resources of electrospun polymers.

2.2. CVD fabrication

CVD is a process in which gaseous reactants react in the gas phase or at the gas–solid interface and are finally deposited into solid substances. It is one of the most commonly used thin film deposition technologies for manufacturing many functional nanomaterials, including graphene, CNTs, CNFs, and others. CVD can use cheap and readily available hydrocarbons such as ethylene, acetylene, propane, and natural gas as raw materials to grow various functional nanomaterials on the surface of metal or metal alloy catalysts. The advantage of CVD is that the diameter, crystallinity, and internal molecular orientation can be customized through precise control over the synthesis conditions. The production of CNFs by CVD shows high efficiency and low cost.

For instance, Cui *et al.* prepared phosphorous doped spiral CNFs by the CVD method using acetylene pyrolysis at 450 °C in the presence of Ni and then thermal annealing. The prepared materials had a clear 3D layered spiral structure with a large specific surface area and they exhibited excellent electrical conductivity.[38] Duan and co-workers synthesized CNFs by cracking acetylene under catalysis.[39] Firstly, carbon microfibers (CMFs) or glass microfibers (GMFs) were soaked in ethanol for 30 min for pre-treatment. Then the Ni/Co catalyst was prepared by solution impregnation and deposited onto the as-prepared CMFs and GMFs. Finally, 3D layered CNFs were prepared by catalytic CVD using acetylene as the carbon source.

3D CNF nanomaterials can also be fabricated by vertical CVD growth of CNFs on various substrates. For instance, Kang *et al.* reported the super-growth of vertically aligned CNFs on Pd thin film through a thermal CVD method.[40] It was found that CNFs with a diameter of about 50 nm were vertically grown on the substrate, as shown in Fig. 2a and b. This was the first time millimeter-scale CNFs had been produced with a vertical structure, which exhibited excellent field emission properties due to the exceptionally high aspect ratio and sharp tip angle of the formed CNFs. Mishra *et al.* demonstrated the plasma-enhanced CVD synthesis of N-doped aligned CNFs on 3D graphene.[41] As shown in Fig. 2c and d, dense CNFs with a length of about 10 μm were formed vertically on the compressed graphene. Control experiments proved that the compressed graphene substrate promoted the formation of a pure carbon hybrid structure without using any buffer layer, thereby increasing the production yield of CNFs to a dense 3D structure. In another case, Klankowski and co-workers presented the production of vertically aligned CNFs on copper foils by using a DC-biased plasma enhanced CVD method.[42] The prepared CNFs had an average length of 3.0 μm and a diameter of 150 nm. To improve the applications of CNFs in energy science, a pure Si layer of 465 nm was coated on the surface of CNFs to form a core–shell structure (Fig. 2e and f). The plasma-enhanced CVD mediated the fabrication of 3D CNFs with a unique microstructure that was

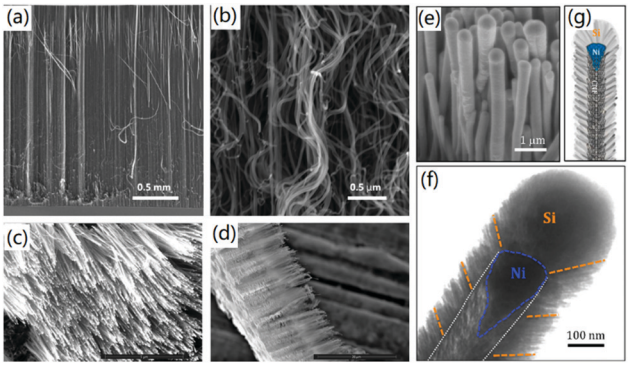

Fig. 2 The CVD-based fabrication of vertically aligned CNFs. (a and b) Vertically aligned CNFs on Pd thin film; (b) is a zoomed image of (a). Reprinted images with permission from ref. 40. Copyright 2014, Elsevier BV. (c and d) CNFs grown on 3D graphene. Reprinted images with permission from ref. 41. Copyright 2019, Wiley VCH. (e–g) Si-Coated vertically aligned CNFs: (e) SEM image, (f) TEM image, and (g) a schematic diagram of the microstructure. Reprinted images with permission from ref. 42. Copyright 2015, Elsevier BV.

similar to a stack of graphitic cones with many graphitic edges at the sidewalls, thereby improving the performance for lithium-ion battery (LIB) applications.

The combination of 3D electron tomography (3D-ET) and high-resolution transmission electron microscopy (HRTEM) provides a successful method for determining the 3D topography with a characteristic size at the nanoscale. Kaneko *et al.* used 3D-ET to characterize the morphology of CNFs grown by bias-enhanced microwave plasma-enhanced CVD, and observed the existence and distribution of a wedge-shaped carbon film composed of amorphous carbon and CNF, and they proposed a growth model. They revealed not only the 3D shape of CNFs, but also the distribution of CNFs at low magnification. It was also agreed that the growth of CNFs was achieved through the decomposition of carbon gas molecules on the surface of the Ni catalyst, and the diffusion of carbon atoms through Ni particles and the subsequent precipitation at the particle/fiber interface.[43]

2.3. Hydrogel/aerogel-based templated synthesis

Hydrogels and aerogels are common 3D network structure gels formed by chemical and physical cross-linking. Aerogels can be called solid smoke, and have ultra-low density and are the lightest solid in the world. Moreover, they have high strength and heat resistance, and can bear thousands of times of their own weight. Therefore, they have potential applications in the fields of energy storage, environmental remediation, strain/pressure sensors, insulators, *etc.* Hydrogels can expand rapidly in aqueous solution, and can maintain a large volume of water content without dissolving. This material with its high water absorption and high water-retention can be used in environmental science, energy storage, sensors, thermal insulators, biomedicine, *etc.*

The preparation of carbon gels consists of three steps: polymerization, drying, and carbonization.[44] Aerogels filled with air can be obtained after wet gel drying. A suitable drying technology can maintain the original porous network structure of the aerogel skeleton. The commonly used drying technologies include mainly supercritical drying and freeze drying.

Supercritical drying is a traditional technology for preparing aerogels. By controlling the temperature and pressure, the solvent reaches its critical point in the drying process. The vapor–liquid interface of the cavity disappears, and the liquid in the gel is eliminated under the conditions of a critical fluid. At the same time, the reticular structure of the gel remains unchanged, forming an aerogel with high permeability and a 3D network structure.[45,46] Freeze drying is a more economical, simple drying method, and is more widely used. First, the liquid in the wet gel is frozen below the freezing point temperature, so that the liquid is changed from the liquid to the solid state, and then sublimated into a vapor at the appropriate vacuum level, so that dry aerogels are obtained. Freeze-drying is widely used because of its simplicity and effectiveness.

The formed 3D hydrogels and aerogels are excellent templates for the fabrication of 3D CNF-based nanomaterials.[47] For instance, Liang and co-workers reported the template synthesis

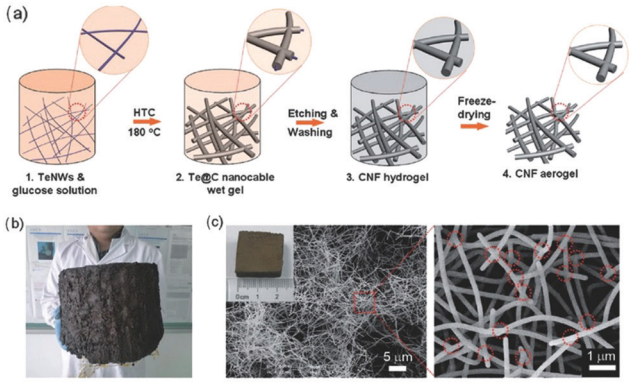

Fig. 3 Templated synthesis of 3D macroscale CNFs: (a) the synthesis mechanism, (b) a photograph of macroscale CNF aerogel with a volume of 12 L, and (c) SEM images of cut small-size CNF aerogels at different magnifications. Reprinted images with permission from ref. 48. Copyright 2012, Wiley VCH.

of macroscopic-scale 3D CNF hydrogels and aerogels.[48] The production process of both hydrogels and aerogels of CNFs is shown in Fig. 3a. Firstly, ultrathin Te nanowires (TeNWs) were dispersed in glucose solution to form a homogenous mixture, which was then treated at 180 °C for 12–48 h to form a robust monolithic gel-like Te/C product. After etching and washing, the TeNWs were removed and CNF hydrogels were created. In a further step, the as-prepared CNF hydrogels were freeze dried into CNF aerogels. This strategy is facile for the production of macroscale CNF aerogels by increasing the volume of the wet gel. For instance, the use of 12 L of monolithic wet gel resulted in the formation of very large aerogels (Fig. 3b) after hydrothermal carbonization and freeze-drying processes. In addition, it is really easy to cut the macroscale aerogels into small pieces with desired shapes. As indicated in Fig. 3c, the SEM characterization of a CNF aerogel with a size of 2 centimetres revealed the nanowire network structure of 3D CNF aerogels. A further zoomed image showed the successful production of highly uniform NFs, which interconnected with each other to a high degree through numerous junctions.

Zhang *et al.* used water-soluble carboxymethyl chitosan (CMCh) hydrogel as a template, and then further cross-linked it with metal cations to form nanofibrous metal polysaccharide coordination precursors.[49] After freeze-drying, carbonization, and low-temperature pyrolysis, 3D CNF structures embedded with various metal CMCh skeletons were formed. Recently, Chen and co-workers demonstrated the production of hierarchically porous N-doped CNF aerogels by using self-assembled bacterial cellulose (BC) gel as a template through freeze drying and carbonization treatments.[46]

2.4. Hydrothermal synthesis

Hydrothermal synthesis is a kind of method that uses water as a solvent in a sealed container to form a relatively high-temperature and high-pressure reaction environment by heating and pressurizing the system, to make the substance dissolve and recrystallize to grow various crystals. Hydrothermal synthesis has

the advantages of simple operation, easy control over reaction conditions, and high yield. It is not only an excellent method to synthesize carbon nanomaterials, but it is also easy to synthesize macro 3D bulk materials.[50,51]

A 3D structure of hydrogels can be formed through self-assembly in a hydrothermal synthesis process.[52,53] The solvothermal rule is to use other liquids instead of aqueous solutions as solvents to solve the problem that some materials are difficult to dissolve in water and insensitive to the change in water state. Different solvents can also be used to control the crystal shape and particle size of nanomaterials.

3D CNF-based nanomaterials could be fabricated through hydrothermal synthesis and corresponding post-treatments. The hydrothermal method has usually been utilized for the synthesis of 3D CNF-based hybrid functional nanomaterials. For instance, Feng *et al.* utilized $Ni(OH)_2$ nanosheets as hard templates and used the hydrothermal method to connect 1D CNFs into a 3D framework in the process of a hydrothermal reaction.[54] During the hydrothermal reaction process, $Ni(OH)_2$ nanosheets were attached onto the surface of CNFs. Meanwhile, added glucose in the hydrothermal reaction was adhered onto the surface of CNFs and then carbonized into carbon nanosheets, as shown in Fig. 4a. The fabricated 3D CNF-based nanomaterials contained numerous 2D carbon nanosheets, which were adsorbed uniformly on the CNFs, as proved by the SEM images in Fig. 4b and c. The corresponding TEM images of the interior structure of the 3D CNF nanomaterials indicated that the CNFs were well-wrapped with vertically oriented carbon nanosheets (Fig. 4d and e). This designed special structure provided favourable conditions for electronic transmission and acted as a physical barrier to inhibit the dissolution of polysulfide, thereby inducing enhanced performance in the fabricated lithium–sulfur batteries.

Ju *et al.* reported the synthesis of 3D porous CNFs loaded with MoS_2 nanoflake-flowerballs *via* a hydrothermal reaction.[55] First, ammonium molybdate thiourea and a certain amount of 3D porous CNFs were mixed in distilled water, and stirred until they were completely dissolved, and then reacted at a high temperature for a period of time to obtain a 3D CNF composite product. The formed 3D CNF-based hybrid nanomaterials had a large reaction area and conductive paths, thereby exhibiting high performance as an anode material for Li-ion capacitors.

In the solvothermal method, the choice of solvent depends on the demands of the reactant. A pure solution or a mixed solution of many substances can be used as the reaction solution.

2.5. Combined strategies for CNF-based 3D materials

In fact, two or more techniques are usually used in the preparation of 3D CNF-based nanomaterials. In the following, we will introduce some cases of fabricating 3D CNFs to help readers understand the combined strategies.

For instance, Alali and co-workers reported the fabrication of 3D hybrid Ni-multiwall carbon nanotube (Ni-MWCNTs)/CNFs nanomaterials *via* combined electrospinning and CVD synthesis.[56] As shown in Fig. 5, previously mixed PAN/PVP precursors were utilized to form PNF mats by electrospinning and then the as-spun PNF mats were carbonized to form a CNF matrix. After that, CVD growth of MWCNTs was applied to fabricate 3D hybrid Ni-MWCNTs/CNFs nanomaterials. The formed CNFs and MWCNTs revealed uniform diameters of 150 and 20 nm, respectively, and the formed 3D hybrid nanomaterials exhibited a large surface area of 530 $m^2\ g^{-1}$ and high performance for sensing sarin nerve agent with a concentration as low as 1 ppm. Most importantly, this combined strategy of electrospinning and CVD for the formation of MWCNTs/CNFs hybrids was economical and effective, and avoided the aggregation of MWCNTs in the fabrication process of 3D nanomaterials.

In another similar study, Lu and co-workers prepared 3D hierarchical CNFs/TiO_2@MoS_2 core–shell heterostructures by electrospinning, hydrothermal reaction and *in situ* growth for the fabrication of 3D CNF-based flexible electrode materials.[57] Electrospun PAN NFs were utilized as templates for the production of CNFs with a uniform structure through carbonization. With an increase in temperature and the loss of nitrogen,

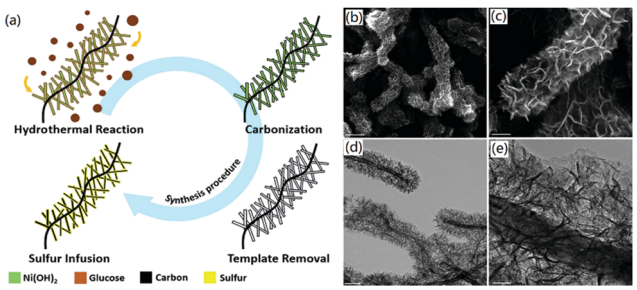

Fig. 4 The one-step hydrothermal synthesis of carbon nanosheet-CNFs as a 3D carbon scaffold: (a) synthesis strategy, and (b–e) SEM and TEM images of 3DCNF. The scale bars are (b) 1 μm, (c) 250 nm, (d) 500 nm, and (e) 100 nm. Reprinted images with permission from ref. 54. Copyright 2017, Royal Society of Chemistry.

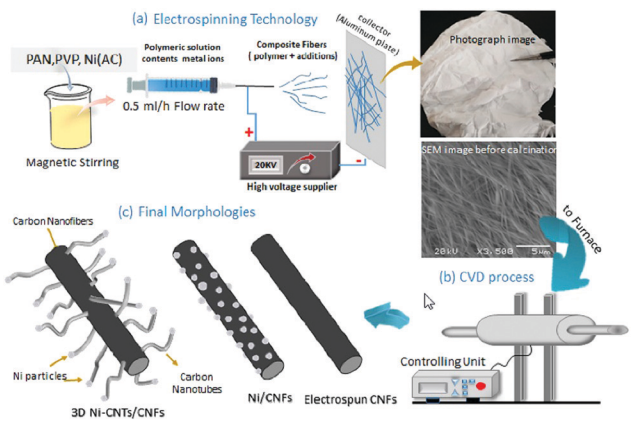

Fig. 5 The production of 3D Ni-MWCNTs/CNFs through electrospinning, CVD, and carbonization: (a) illustration of the synthesis processes, preparation of the solution, and electrospinning with photographic and SEM images of the as-spun mat, (b) the CVD unit, and (c) the expected morphologies of electrospun CNFs, composite Ni/CNFs, and hybrid 3D Ni-MWCNTs/CNFs. Reprinted images with permission from ref. 56. Copyright 2019, Elsevier BV.

a large number of pores are produced on the surface of the CNFs. In addition, TiO_2 and MoS_2 were used to modify the CNFs *via* an *in situ* synthesis. The fabricated CNF-based 3D nanocomposite exhibited promising applications in energy storage systems and wearable, portable nanodevices. Dahal and co-workers prepared porous CNFs by electrospinning PAN and zeolitic imidazolate framework (ZIF-8) NPs.[58] Electrospinning and simple carbonization with PAN and ZIF-8 as precursors is a simple and effective way to synthesize 3D CNF networks with voids and hollow channels on the surface. The obtained NF felt is then treated with sodium borohydride aqueous solution and freeze-dried to maintain the 3D structure and cross-linking of the CNF network.

Recently, Lv and co-workers reported that a 3D network CNF aerogel embedded in ultrafine FeSe NPs was synthesized through a sustainable seaweed-template strategy.[59] Sodium alginate, which can form an ''eggshell'' structure after ion exchange with Fe^{3+}, is the key to the synthesis. The alginate was mixed into ferric chloride solution to form a cross-linked gel with iron, and then the gel was separated and washed and the as-prepared gelation was dehydrated *via* a freeze-drying process to obtain 3D Fe-alginate aerogels. The prepared aerogels were heated and pyrolyzed in Ar gas to obtain FeSe-CNFs, and then postprocessing was used to remove metals and finally CNF aerogels were obtained.

2.6. Summary of the fabrication of 3D CNF nanomaterials

Based on the above introduction, it is found that processes such as electrospinning, CVD, templated synthesis, and hydrothermal synthesis are useful for the successful synthesis of 3D CNF nanomaterials. The electrospinning technique has been the most facile and most direct way to create 3D PNF scaffolds, which could then be post-treated through calcination or carbonization to form 3D CNF nanomaterials. This method can be utilized for the fabrication of various smooth, porous, heteroatom-doped, and NP-decorated CNFs with improved properties. However, for the formation of CNFs, high voltage and high temperature are usually needed in the synthesis process. With the CVD method, it is possible to produce high-quality and highly crystallized CNF on metals or other carbon materials (such as graphene) substrates. Sometimes, 3D CNF arrays could be fabricated to form uniform structures, but catalysts are needed for the growth of CNFs and complex experimental conditions. In addition, it needed a high consumption of energy.

The templated synthesis combined with carbonization provides a direct and simple way to fabricate 3D CNFs with uniform structures. In this case, some natural or synthetic nanofibrous materials (such as cellulose or chitosan NFs) have been fabricated into 3D hydrogels by chemical or physical cross-linking, which were then freeze-dried and carbonized to form 3D CNF aerogels. This method can make full use of natural biomass materials to achieve their high-performance reutilization. However, the types of natural nanofibrous materials are limited. In addition, the formation of carbon aerogels will consume a lot of energy.

The hydrothermal synthesis has exhibited great advantages for the production of various CNF-based hybrid 3D nanomaterials with synergistically improved properties. This technique is useful for the decoration of the as-prepared CNFs with various metal and metal oxide NPs to realize multiple functions. The template and hydrothermal synthesis could be combined with the

Table 1 Summary of the fabrication of CNF-based 3D nanomaterials

Method	Precursors	CNF material	Functions/applications	Ref.
Electrospinning	ZIF-67/PAN	Co-Decorated N-CNFs	Li–S batteries	33
Electrospinning	PAN	3D CNFs	Li-Based batteries	34
Electrospinning	PVP/AB	3D porous N/B-doped CNF network	High catalysis performance/batteries	35
Electrospinning	Montmorillonite/PAN	3D CNFs	Electrochemical sensors	36
Electrospinning	PAN/cobalt salt	Co@3D-CNFs	Supercapacitors	37
CVD	Acetylene	Phosphorus-helical CNFs	Electrochemical sensors	38
CVD	Acetylene	3D CNFs/microfibers	Fuel cells, sensors, catalysis	39
CVD	C_2H_4	Vertically aligned CNFs	Field emission	40
CVD	Methane	Aligned N-CNFs/graphene	Supercapacitors/sensors/batteries	41
CVD	Methane	Vertically aligned CNFs	Nanoscience and nanotechnology	43
Hydrogel/aerogel-based templated synthesis	Carboxmethyl chitosan	Co_3O_4@N-CNFs	Lithium and sodium storage	49
Hydrogel/aerogel-based templated synthesis	Cellulose/ZIF-8 gel	N-Doped CNF aerogels	All-solid-state supercapacitors	46
Hydrothermal synthesis	$Ni(OH)_2$ nanosheets/CNFs	Carbon nanosheet-decorated CNFs	Lithium–sulfur batteries	54
Hydrothermal synthesis	PVA/PTFE	3D porous CNFs/MoS_2	Li-Ion capacitors	55
Electrospinning and CVD fabrication	PAN/PVP	3D Ni-MWCNTs/CNFs	Gas sensors	56
Electrospinning and hydrothermal synthesis	PAN/terephthalic acid	CNFs/TiO_2@MoS_2	Electrochemical electrode materials	57
Electrospinning and hydrothermal synthesis	PAN/ZIF-8	3D CNF networks	Supercapacitors	58
Templated synthesis and hydrothermal synthesis	Alginate aerogel/$FeCl_3$	CNF–FeSe aerogel	Na storage	59

electrospinning and CVD methods to create multifunctional CNF-based nanomaterials.

Table 1 summarizes the type of materials and the synthesis strategies of various CNF-based 3D nanomaterials that have been introduced above.

3. 3D CNF nanomaterials for energy applications

CNF-based 3D nanomaterials have exhibited wide applications in energy storage and clean energy production due to their porous structure, high specific surface area, numerous active sites, and good catalytic properties. In this section, the energy science applications of CNF-based 3D nanomaterials in supercapacitors, fuel cells, electrochemical batteries, and electrochemical hydrogen evolution are presented.

3.1. Supercapacitors

Supercapacitors are high-performance energy storage devices that can be used as a complementary substitute for chemical batteries. Supercapacitors have the advantages of fast charging speed, long cycle life, and large electrical capacity. Currently, the design of nanostructures with suitable dimensions and the construction of highly effective electron/ion transport channels are crucial for fabricating high-performance supercapacitors for practical applications.

CNFs have been widely utilized for the fabrication of supercapacitors due to their superior physical and chemical properties, such as large surface area, high conductivity, good temperature stability, and low cost. In addition, in order to achieve high ratio capacitance, high rate capability, and good cycle stability of the fabricated supercapacitors, many studies have been carried out to produce CNF-based 3D nanomaterials for supercapacitors. 3D CNFs not only have the characteristics of CNFs, but also show better performance in electronic transmission than pure CNFs.

1D CNF is a kind of electrode material with high performance and low cost, but its relatively low surface area and limited ion diffusion and transport channels inhibited its further development, which can be successfully solved by the fabrication of 3D CNFs. In order to further obtain high specific capacitance, high rate capability, and good cycle stability, many efforts have been made to manufacture a functional 3D CNF network through appropriate heteroatom doping and surface modification.[58,60] In addition, if B, N, S, and other elements are doped on/in CNFs, the rate capacity and cycle stability of the electrode materials can be effectively enhanced. These positive effects may be ascribed to the introduction of hydrophilic elements to improve the wettability of the electrode, the enhancement in conductivity by charged carriers, and the increase in electronic density to improve the capacitance.

Carbon aerogels have the characteristics of low density, high porosity, a 3D interconnecting CNF network structure, stable mechanical properties, good conductivity, and low cost. Moreover, their 3D network has a large number of holes, which could greatly promote the penetration and diffusion of ions and lead to further uses for energy storage and conversion.[61] For instance, Chen *et al.* reported the fabrication of free-standing N-doped CNF aerogels with a hierarchically porous structure, which exhibited potential applications for all-solid-state supercapacitors.[46] As shown in Fig. 6a, a piece of BC was immersed in 1% NaOH, and then Zn^{2+} ions and 2-methylimidazole (2-MeIM) were added to form BC@ZIF8 hybrid nanocomposites. The as-prepared nanocomposites were freeze-dried to obtain BC@ZIF8 hybrid aerogels, which were then carbonized to fabricate highly conductive N-doped CNF aerogels. BC was selected for the fabrication of CNFs because of its uniform fibrous structure, low cost, large resource, and the green synthesis of 3D aerogels by freeze-drying. In addition, BC-based CNF aerogels provided self-N-doping and the formation of attractive free-standing electrode materials with high performance and durability. To fabricate a symmetrical supercapacitor (SSC), two identical CNF aerogel electrodes were connected together with a cellulose paper separator. The electrochemical tests indicated that the galvanostatic charge/discharge curves of the SSC cycled at different current densities were linear and symmetrical, proving the outstanding capacitive performance of the fabricated SSC. In addition, the fabricated all-solid-state SSC exhibited excellent capacitance retention by retaining 91% of the initial value after 5000 cycles (Fig. 6b). For practical applications, an LED could be powered by two supercapacitors in series. Compared to previously reported data, the fabricated SSC had higher power density and relatively high energy density, as shown in Fig. 6c. The improved capacitance was ascribed to the 3D porous structure and high conductivity of the

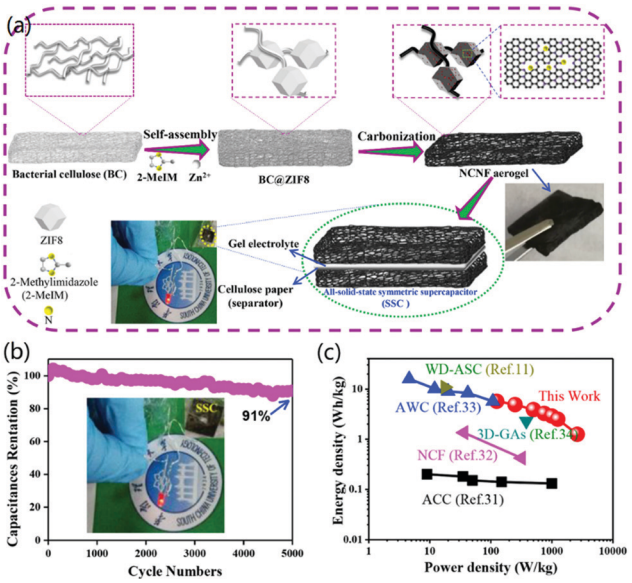

Fig. 6 3D CNF aerogels for supercapacitor applications. (a) BC-based self-assembly, hydrothermal reaction, and carbonization for the synthesis of N-doped CNF aerogels. Two CNF aerogel electrodes were connected with one cellulose paper to form an SSC. (b) Capacitance retention and cycling performances of the SSC. (c) Comparison of both energy density and power density with other capacitors. Reprinted images with permission from ref. 46. Copyright 2019, Elsevier BV.

designed aerogel material. Therefore, the designed BC-based 3D CNF aerogels were highly beneficial for the fabrication of low-cost, environmentally friendly, and scalable electrode materials for SSCs with improved performance. In other cases, electrospun 3D CNF@MnO_2 and pyrolyzed CNF/graphene oxide (CNF/GO) aerogels have been synthesized successfully for asymmetric and compressible supercapacitors, respectively.[62,63]

In addition, the lightweight elastic CNF aerogel developed in recent years revealed potential applications in wearable supercapacitors due to its low density and high mechanical strength. For instance, Zhang and co-workers prepared CNFs from electrospun PAN NFs as raw materials under the action of polyvinylpyrrolidone (PVP). Then the CNF-based aerogels were prepared by freeze-drying and carbonization, which were then activated by carbon dioxide and served as anode materials for supercapacitors.[64] The optimized aerogel anode material had the advantages of high conductivity, good elasticity, and strong mechanical strength, meanwhile still maintaining the large capacitance of carbon nanomaterials.

Besides 3D CNF aerogels, 1D CNFs could be composited with other nanomaterials to construct 3D CNF-based hybrid nanostructures to improve the performance and efficiency of carbon nanomaterials used in electrochemical devices.[65–68] For example, Lin and co-workers grew CNFs on a 3D graphene network (3DGN) and successfully constructed CNFs/3DGN hybrid nanomaterials, which greatly increased the surface area of the electrode materials.[65] To maximize the specific surface area and boost the electrochemical reactions of the electrode materials, they first synthesized 3DGN by thermal CVD and then used a pulse-mode electrochemical deposition technique to grow CNFs on 3DGN. The formed CNFs/3DGN exhibited a very large surface area, an excellent substrate for binding CNFs, and good vertical/horizontal electron transmission ability, and could therefore be a promising candidate for the fabrication of high-performance supercapacitors. In this process, the key was the pulse-mode electrochemical deposition technique and the Ni NP catalyst for CNF growth. The CNFs/3DGN hybrid nanostructure exhibited good specific capacitance and cycle stability, and was expected to become a low-cost candidate material for high-performance supercapacitors. Qiu *et al.* reported the synthesis of vertically aligned CNTs on CNFs for the fabrication of a hierarchical 3D carbon nanomaterial for flexible supercapacitors.[66] The fabricated supercapacitors exhibited a high specific energy and ultrahigh energy density. In addition, the capacitors had super-long charging/discharging cycles (20 000 times), retaining about 97.0% electric double layer capacitance. This excellent performance was ascribed to the roles of vertically aligned CNTs in storing and accumulating charge and the CNF backbone for transporting charge. In another case, Lai and co-workers demonstrated the preparation of 3D Ni–Co layered double hydroxide nanorods (Ni–Co LDHNRs) on electrospun carbonized NFs, which also revealed high electrochemical performance for supercapacitors.[68]

3.2. Fuel cells

A fuel cell is an environmentally friendly and efficient energy converter, which converts chemical energy into electrical energy through electrochemical reaction. The reaction consists of two separate semi-reactions: the oxidation of the anode and the reduction of the cathode. At present, most commercial fuel cells work with Pt-based electrocatalysts. However, the low reserves and high price of Pt catalysts have restricted their wide applications and the further commercialization of fuel cells.

CNFs have been utilized as catalyst carriers to support Pt and other redox catalysts for fuel cells due to their advantage in mediating electron transfer.[69] This kind of CNF-based catalyst can provide more active sites and stronger electrochemical activity, reducing the consumption of precious metal catalysts and improving their service life.[70,71] In addition, the non-metallic catalysts derived from CNFs have the advantages of low price, stable performance, and high redox activity, showing high potential to replace expensive catalysts for the redox reaction of fuel cells.[72,73]

Due to the disordered carbon structure of electrospun CNFs, more active sites can easily be introduced to promote the chemical adsorption of oxygen and electrochemical reactions, which are beneficial to the redox reaction of fuel cells. However, the collective behavior of the electrochemical system depends strongly on the spatial distribution of the active sites and the nature and intensity of the interaction between the active sites, Due to the overlapping of electrospun CNFs, the contact resistance is large, which will limit the charge transfer. To overcome this problem, some strategies, such as the doping of CNFs with heteroatom elements to reduce the cross-linking resistance[74] or building a 3D network structure, have been adopted to improve the conductivity and obtain more active sites.[16]

For instance, Chen *et al.* demonstrated the production of nonwoven 3D CNFs *via* an electrospinning method for application as electrodes in microbial fuel cells.[75] The fabricated 3D CNF-based electrodes exhibited excellent performance for bioelectrochemical systems such as microbial fuel cells and microbial electrolysis cells. In order to prepare an electrode with good electrical conductivity, high biocompatibility, chemical stability, and large surface area for microbial fuel cells, Khare and co-workers reported the fabrication of CNF-skinned 3D Ni/carbon micropillars with a laser-ablation technique, and proved that the 3D CNF-based materials had promising potential for microbial fuel cells.[76] As shown in Fig. 7, the CNF-skinned electrode revealed a uniform microstructure with arrays of micropillars, which could increase the formation of biofilm and promote microbial interaction with the electrode. Therefore, the generated microbial fuel cells exhibited a high open circuit potential of about 0.75 V and a maximum power density of about 2496 mW m^{-2}. The obtained results indicated that the high performance could be ascribed to the synergistic effects of graphitic CNFs, the high catalytic activity of N-doping and Ni NPs, and the support of the designed 3D microstructure for the biofilm. In addition, the utilization of Ni NPs as catalysts for the CVD production of CNFs enhanced the electronic conductivity of the designed materials.

Shi *et al.* demonstrated the synthesis of a B/N-doped porous CNF web with a self-designed multi-needle electrospinning setup.[77] It was found that the formed CNFs had a micro-mesoporous

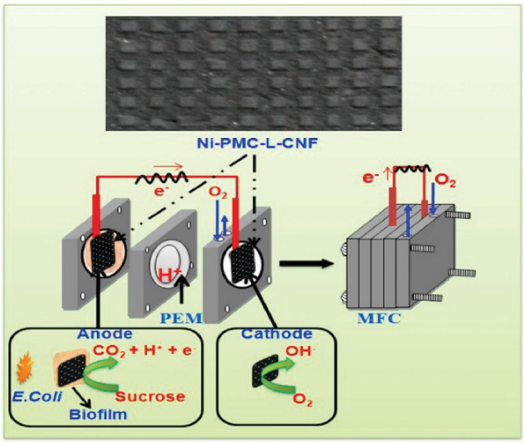

Fig. 7 CNF-skinned 3D Ni/carbon micropillars for microbial fuel cell applications. Reprinted images with permission from ref. 76. Copyright 2016, Elsevier BV.

structure and void spaces for facilitating mass transport. In addition, the co-doping of B and N into CNFs improved the metal-free catalysis toward the oxygen reduction reaction (ORR) in alkaline media, identifying the commercial application of the designed 3D CNF-based nanomaterials in fuel cells.

3.3. Electrochemical batteries

3D CNF-based nanomaterials can also be utilized as electrode materials for electrochemical batteries. In this section, typical applications of 3D CNF materials in LIBs, Na-ion batteries (NIBs), and K-ion batteries (KIBs) are presented and discussed.

3.3.1. Application in LIBs. LIBs have been widely used to provide power for notebooks, mobile phones, e-vehicles, and other electronic devices. Their performance is closely related to the electrode materials used in the batteries. CNFs are a common material for the preparation of the cathode for LIBs due to their good conductivity, high specific surface area, and porous structure, endowing the prepared batteries with good capacity and recyclability.[78–80]

Recently, more efforts have been expended to develop LIBs with excellent electrochemical performance, including higher energy density, higher power density, and better cycle stability, to meet the high requirements for the high energy consumption of various electric devices. It has been found that the fabrication of a 3D CNF structure produced a large accessible active surface area and efficient carbon active sites, which were ideal for promoting electrolyte permeation, accelerating electron transfer, and limiting volume expansion to improve the performance of batteries.[81] The use of a 3D CNF matrix as the substrate material is an effective way to solve the problem of the lithium metal deposition/dissolution cycle. For instance, Matsuda found that the conductivity of CNFs was an important factor determining the deposition behavior of Li^+ in 3D CNF matrices.[34] In the study, the author compared the practical application of 3D CNFs with different conductivities in LIBs. It was found that a 3D matrix with highly conductive CNFs provided a pathway for electron transfer, and promoted the deposition of Li metal at the outer surface of the matrix, thereby improving the battery performance a great deal. In another case, Ju and co-workers prepared a 3D porous CNF composite loaded with MoS_2 nanosheets by a simple hydrothermal method for high-performance Li-ion capaciors.[55] In that case, MoS_2 nanosheets provided more active sites for the reaction, while 3D porous CNFs provided excellent electron transport channels.

To solve the problem of the weak interaction between the active materials and conductive CNF matrix and to improve the long-term application of electrode materials, Zhang and co-workers recently demonstrated the construction of ultrafine metal oxides (MO, Co_3O_4, Mn_3O_4, and Fe_3O_4) on N-enriched 3D CNFs through the formation of a metal-carboxymethyl chitosan (CMCh) framework and a subsequent annealing process.[49] The strong coupling between the MO and CNFs promoted fast reaction kinetics and enhanced the structural stability of the final 3D materials, as shown in Fig. 8a. Therefore, the fabricated 3D MO@CNFs materials exhibited high capacity and stable Li^+ storage. For instance, the prepared Co_3O@CNFs revealed a high Li^+ storage capacity of 1199 mA h g^{-1} at 200 mA g^{-1} and a good cycling lifespan, as well as high capacity retention. This work presented a facile strategy to construct 3D CNF-based hybrid nanomaterials by using sustainable polymer hydrogels for high-performance Li-ion storage.

Besides LIBs, Li-ion based secondary batteries, such as Li–S batteries, have also attracted more attention recently. 3D CNF-based nanomaterials have also been utilized to fabricate high-performance Li–S batteries. For instance, Yao and co-workers reported the electrospinning synthesis of a 3D CNF network decorated with metal Co, and its further applications for Li–S batteries.[33] In their study, the as-prepared 3D Co/N-CNFs

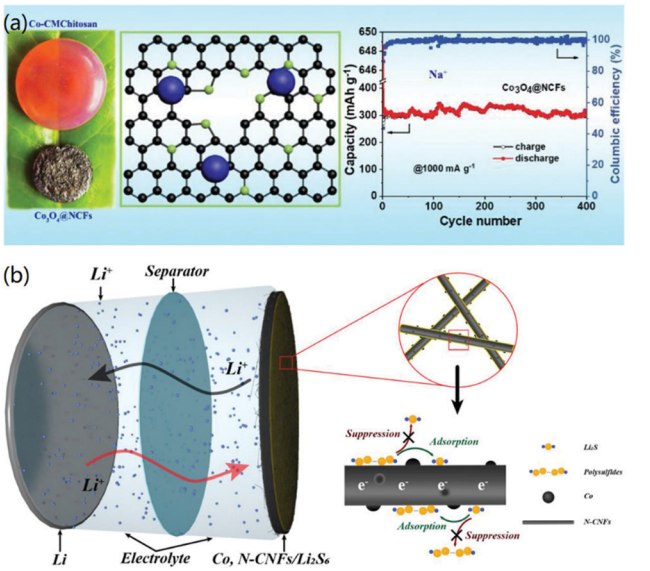

Fig. 8 3D CNF-based nanomaterials for Li-batteries. (a) 3D metal oxide@N-CNFs for LIBs. Reprinted images with permission from ref. 49. Copyright 2020, Elsevier BV. (b) 3D Co-decorated N-CNF network for Li–S batteries. Reprinted images with permission from ref. 33. Copyright 2020, Elsevier BV.

network membrane was used as the positive current collector containing Li_2S_6 for Li–S batteries, as shown in Fig. 8b. It was found that the synthesized 3D CNF materials had synergistic effects for improving the battery performance: the adsorbed Co metal facilitated the uniform nucleation of Li_2S on the surface of the 3D CNF materials, and the 3D structure reduced the overpotential of Li_2S to polysulfides, inhibited the shuttling of LiPS, and prevented the corrosion of the Li anode in the electrochemical reaction process.

In another case, in order to reduce the shuttle effect caused by the high solubility of LiPS, Shang *et al.* demonstrated the synthesis of freestanding Mo_2C-decorated N-CNFs for use as 3D current collectors for Li–S batteries.[82] Both experimental and theoretical studies proved that Mo_2C possessed strong and stable interaction affinity to LiPS, thus alleviating the shuttle effect. In addition, the 3D interconnected nanofibrous structure of the designed materials mediated high electronic conductivity, structural integrity, and fast reaction kinetics, resulting in a promising battery performance with high specific capacity and long-term cycling stability.

3.3.2. Application in NIBs. NIBs rely on the movement of Na^+ between the positive and negative electrodes to transfer electrons. In nature, Na^+ is very abundant and easier to obtain than Li^+, and therefore it is an excellent substitute for LIB. In order to realize the high rate capability of NIBs, it is necessary to build an electrode with a small ion diffusion distance, high Na^+ diffusion coefficient, and fast electron transmission speed, by which both electrons and Na^+ can be rapidly transmitted to the active materials. CNFs and CNFs doped with N, S, tin, and other elements have previously been synthesized and utilized for the fabrication of NIBs.[83–85]

The function of CNFs in NIBs is similar to that in LIBs. They are all used as electrode materials to improve the electron transfer rate and enhance the conductivity of the electrode. However, Na^+ has a larger ion radius than the lithium ion, so a larger layer spacing of the matrix material is usually needed to accommodate and transport Na^+. A 3D interconnected CNF structure can not only promote the migration of Na^+, but also improve the structural stability of the CNF electrode and alleviate the volume change in electrode materials during the charging and discharging process, showing potential applications for the fabrication of novel NIBs.[86,87] For instance, Wang and co-workers reported the synthesis of 3D interconnected CNF thin films co-doped with B and N (BN-CNFs) to achieve high specific capacity and a remarkably high rate capacity.[86] The N doping could improve the reactivity and electronic conductivity of CNFs and the B doping created more active sites and also enhanced the conductivity of CNFs. Therefore, the synergistic effects of dual-atom doping in CNFs resulted in the increased energy density and power density of the fabricated batteries. As shown in Fig. 9, the BN-CNFs were produced with bacterial cellulose as templates *via* a freeze-drying and carbonization process. The formed 3D porous structure, large surface area, enlarged carbon layer spacing, and B/N co-doping all contributed to the improved NIB performance due to their synergistic effects.

In order to extend the NIB applications, 3D CNF nanomaterials decorated with various metal sulfide/oxide and bimetal NPs have

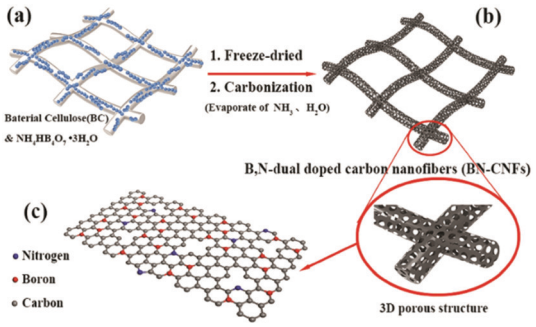

Fig. 9 Fabrication process of a BN-CNFs electrode for NIBs. Reprinted images with permission from ref. 86. Copyright 2017, Wiley VCH.

been utilized.[59,88] Iron sulfides and oxides are often doped in 3D CNFs as electrode materials. Such structures not only retained ion transport channels, but also enhanced the conductivity of electrode materials, which were conducive to the diffusion of Na^+ and improved the cycling stability of the materials. The functional NPs with high catalytic properties were embedded in porous CNFs to form a flexible 3D network structure. The prepared electrode materials revealed good performance and cycle stability, and are promising electrode materials for NIBs.

3.3.3. Application in KIBs. The KIB is another alternative battery which can replace LIB in some applications. The higher electrode potential of K^+ can induce a stronger working voltage and higher energy density than that of Li^+. CNFs can also be utilized for the fabrication of KIBs through enhancing the conductivity, stability, and sustainability of electrode materials to increase the battery capacity.[89–91] However, similar to NIBs, the large ion radius of K^+ results in slow transmission speed and poor storage capacity, which affect the cycle life of the battery. Therefore, it is necessary to develop a new type of K^+ storage material to overcome these problems.

The preparation of high-throughput, high specific surface area 3D frameworks from graphene and CNFs as efficient and stable potassium storage materials has attracted a lot of attention.[92,93] In addition, the 3D carbon frameworks doped with N, silica NPs, MoO_2, or SnO_2 have been fabricated to further improve the performance of KIBs.[94–96]

To improve the poor rate performance and low cycle life of KIBs caused by the large ionic radius of K^+, Zhang and co-workers presented the decoration of hollow N-CNFs (N-HCNFs) with $NiCo_2S_4$ nanorods for the synthesis of 3D nanomaterials for KIBs.[97] As indicated in Fig. 10a, $NiCo_2S_4$@N-HCNFs were synthesized through electrospinning, high-temperature carbonization, and hydrothermal reaction. The corresponding SEM image proved that uniform tapered rod-like $NiCo_2S_4$ were formed on the outer surface of HCNFs. The fabricated KIB exhibited a capacity of 263.7 mA h g^{-1} after 200 cycling tests (Fig. 10b), and the rate performance showed improved values compared with both HCNFs and $NiCo_2S_4$@N-CNFs (Fig. 10c). In addition, the galvanostatic charge/discharge curves with the first 5 circles indicated that excellent cycle stability of the designed electrode materials (Fig. 10d). In the KIB tests, it was found that the designed structure not only shortened the ion transport distance,

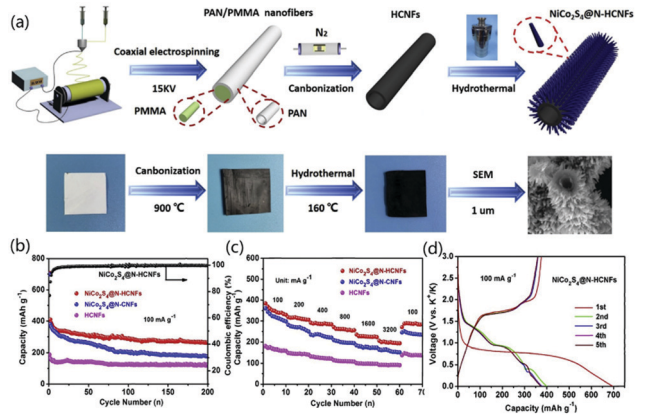

Fig. 10 $NiCo_2S_4$@N-HCNFs for KIB applications: (a) synthesis mechanism, (b) cycling performance, (c) rate performance at various current densities, and (d) galvanostatic discharge/charge curves. Reprinted images with permission from ref. 97. Copyright 2020, Elsevier BV.

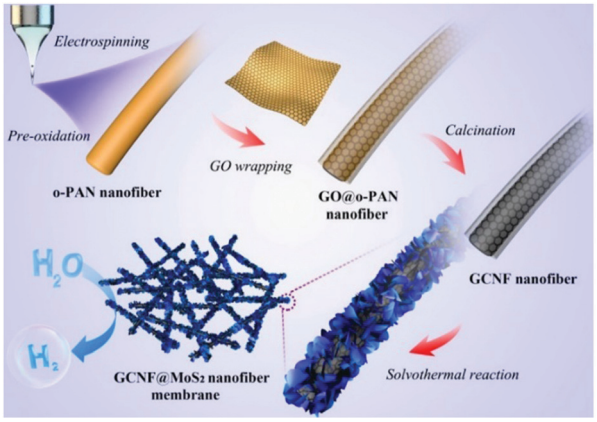

Fig. 11 Fabrication of graphene-wrapped CNFs-decorated with MoS_2 for HER applications. Reprinted images with permission from ref. 103. Copyright 2016, Elsevier BV.

but also increased the contact area with the electrolyte, which effectively improved the electrochemical performance. Due to the hollow structure of CNFs and the decoration with bimetallic sulfide, the synthesized $NiCo_2S_4$@N-CNFs exhibited excellent mechanical properties as well as improved ion transport efficiency and electronic conductivity, which were useful for promoting their potential applications as a negative electrode material for KIBs.

Although KIBs have good application prospects, the current study is still in the preliminary stage, and the development of 3D CNF-based functional electrode materials with high performance, high stability, and low cost still is still needed.

3.4. Electrochemical hydrogen evolution

Hydrogen, as a kind of clean and renewable energy, is a substitute for fossil fuels and has broad application prospects. At present, the electrolysis of water has been the most widely used method to prepare hydrogen. In order to improve the efficiency of water decomposition and energy utilization, various functional nanomaterials have been developed as catalysts for electrochemical hydrogen evolution.[98,99]

CNFs have contributed to the production of hydrogen through the electrochemical hydrogen evolution reaction (HER) due to their interconnected structure, high surface area, numerous active sites, and strong chemical stability.[100–102] In the process of HER, the bubbles produced at the solid–liquid interface may block part of the electroactive surface area and affect the reaction rate. The introduction of pores, cracks, and channels in the electrode structure provide potential ways to inhibit the formation of bubbles and promote their separation. CNF-based 3D porous electrode materials can meet all these kinds of needs.

For instance, Gu and co-workers demonstrated the synthesis of advanced CNF-based 3D electrocatalysts for high-performance HER to produce hydrogen.[103] As shown in Fig. 11, PAN precursors were first oxidized and electrospun into oxidized PAN (O-APN) NFs, which were then wrapped with GO nanosheets to form GO@O-PAN NFs. After calcination and subsequent hydrothermal reaction, MoS_2 particles were formed on the graphene-wrapped CNFs (GCNFs), and finally 3D GCNF@MoS_2 NF membranes were created. In this novel 3D structure, graphene functioned as a bridge to link CNFs to form a 3D network and provided highly conductive pathways for facilitating electronic transport. In addition, CNFs acted as excellent spaces between graphene layers for inhibiting their restacking and improving the superior electronic conductivity of graphene. Therefore, this designed 3D material exhibited remarkable electrocatalytic activity with low onset potential, small Tafel slope, large current density, and high stability.

To improve the electrocatalytic performance of CNF-based 3D nanomaterials, various noble and transition metallic NPs have previously been utilized to combine with CNFs to form hybrid 3D nanomaterials.[104–106] For instance, Mi and co-workers prepared a 3D CNF aerogel with biological bacterial cellulose, and then dispersed Pt NPs onto the surface of CNFs to form a CNF/Pt NPs hybrid aerogel.[104] The high conductivity, abundant surface area, and porous structure of the 3D CNFs promoted the mass transfer and hydrogen evolution in the reaction process as a catalyst. In another study, Cao *et al.* demonstrated the fabrication of a 3D porous CNF network decorated with Co nanospheres *via* templated synthesis, freeze-drying, carbonization, and *in situ* chemical synthesis, which resulted in 3D fibrous nanomaterials with abundant channels and interfaces for improving both mass transfer and oxygen evolution.[105] In another similar study, Li and co-workers embedded Co and C_OP NPs into N-doped 3D CNFs by electrospinning and post-heat treatment.[106] The synthesized catalyst also showed excellent catalytic activity and a long service life for the HER. It is clear that the replacement of noble metals with cheap transition metals for the HER to promote water splitting shows great potential in the production of hydrogen with low cost and high efficiency in the future.

4. 3D CNF nanomaterials for environmental science applications

3D CNFs can also be used in environmental science by utilizing their mesh structure, and mechanical and electrical properties.

In this part, we introduce the application of 3D CNFs in applications to water purification, CO_2 capture, and shielding against electromagnetic radiation pollution.

4.1. Water purification

Industrial wastewater from textiles, pharmaceuticals, batteries, dyes, agriculture, and other industries often contains a large number of pollutants, such as organic compounds, pesticides, heavy metal ions, and other inorganic chemicals. It is difficult to purify the industrial wastewater through traditional separation techniques due to the complexity of the wastewater systems.

Water treatment technology based on the adsorption of adsorbents is one of the most popular and widely used water purification methods. The use of adsorbents for treating wastewater has the advantages of high efficiency, low cost, and simple operation, and thus it has been widely adopted in recent years. Carbon nanomaterials, especially graphene and its derivatives have been widely used for the design and synthesis of various adsorbent materials.[107,108] In addition, CNTs,[109,110] CNFs,[110,111] fullerenes,[112] and graphite[113] have also shown promising applications for this aim.

3D carbon nanomaterials have porous structures, a large specific surface area, high permeability, low density, high chemical stability, easy regeneration, and long service life to make advanced adsorbents. The preparation of 3D CNF-based nanomaterials with high porosity is an effective way to improve the adsorption performance of an adsorbent and realize the large-scale application of carbon nanomaterials for water treatment in industry.[114]

Here we would like to present several examples of using 3D CNF nanomaterials for oil/water separation, the adsorption of heavy metal ions and dyes, and capacitive deionization.

To make full use of styrofoam (SF), a polystyrene polymer produced from styrene, and reduce its hazardous effects on the environment, Baig and co-workers synthesized super hydrophobic and lipophilic CNF-incorporated SF (CNF/SF) materials to achieve the efficient separation of oil and water.[115] The interaction between CNFs and SF greatly improved the surface hydrophobicity. In addition, due to the growth of polystyrene on the surface of CNF, a large number of 3D cavities with micropores and macropores were formed, as shown in Fig. 12. Through the combination of two materials, the surface became dense and porous with improved hydrophobicity, and an SF with low dispersion on the surface of the material exhibited good oil/water separation performance. This interesting study brought out two important effects on the fabrication of low-cost but high-performance adsorbents for water purification. Firstly, it revealed the potential of using biomass waste for producing useful functional nanomaterials for treating chemical pollution. Secondly, it provided a novel strategy for creating 3D CNF materials with a simple and environmentally friendly technique, which could be further used in many other fields.

Shen and co-workers demonstrated the construction of 3D hierarchical materials by combining CNFs into graphite felt (GF) supports.[116] Through adjusting the reaction time, physico-chemical properties, such as the surface area, density, porosity,

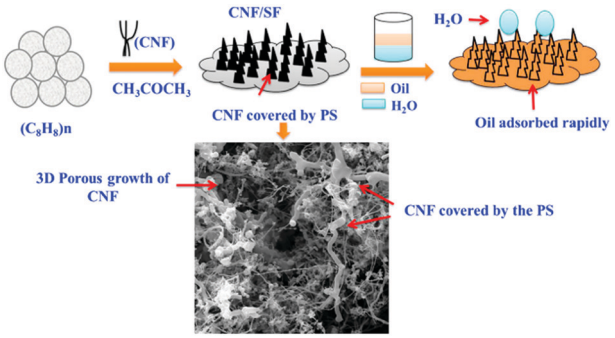

Fig. 12 The design and synthesis of a 3D porous CNF/SF network for oil/water separation applications. Reprinted images with permission from ref. 115. Copyright 2019, Elsevier BV.

and pore structure of the 3D CNF-GF materials, could be tuned effectively. Due to these unique properties, the designed 3D CNF-GF materials exhibited wide water purification applications for removing Pb^{2+}, Congo red, organic solvents, and oils from aqueous solutions with high adsorption capacities, recovery, and recyclability.

In other aspects of water purification, capacitive deionization of seawater has been one method to obtain available fresh water, and 3D CNFs have exhibited promising application prospects in this field. For instance, Liu *et al.* synthesized a CNF-reinforced 3D porous carbon polyhedral network through electrospinning and subsequent carbonization, which could be utilized for capacitive deionization with a high capacity of 16.98 mg g^{-1} at 1.2 V in 500 mg L^{-1} NaCl solution.[117] Zhu *et al.* successfully prepared nitrogen doped CNF aerogels by using bacterial cellulose in NH_3 after freeze-drying and heat treatment.[45] This material has the advantages of high capacitance and low resistance and is a promising candidate for seawater desalination with capacitive deionizing technology. In another study, Li and co-workers designed porous, interconnected, well-organized, and phosphorus-doped 3D CNF aerogels derived from bacterial cellulose for capacitive deionization.[118] The synthesized materials exhibited a high electrosorption capacity of 16.2 mg g^{-1} in 1000 mg L^{-1} NaCl solution.

4.2. CO_2 capture

At present, a large number of greenhouse gas emissions are aggravating global warming and pose a worrying threat to the environment and public health. Among all the greenhouse gases, CO_2 comes from a wide range of sources and has a huge impact on the world climate. Currently, two conventional technologies for CO_2 capture, chemical adsorption by different amines and physical adsorption by a solid adsorbent, have been utilized for the capture of CO_2. However, absorption by ammonia has the disadvantages of high regeneration cost, high toxicity, volatility, and corrosion. In addition, the energy consumption of chemical adsorbents is seriously high during regeneration,[119] which limits their large-scale application. Porous solid adsorption is considered to be one of the most economical and effective methods for CO_2 separation. The key to the success of adsorption technology is large adsorption

capacity, high selectivity, easy regeneration, and stable performance.

CNFs have been thought to be one of the best choices for capturing CO_2 because CNFs not only have the inherent characteristics of carbon nanomaterials, but can also provide an adjustable porous structure.[120,121] In addition, their excellent conductivity is also beneficial to the post-treatment of absorbed CO_2.[122,123] Therefore, CNF materials with high porosity and a 3D structure have wide application prospects in CO_2 adsorption.

For instance, Li *et al.* successfully prepared N-doped porous CNF webs by one-step carbonization activation treatment on an as-synthesized polypyrrole (PPy) NF network.[123] PPy has high N content and a high amount of carbonaceous residue after pyrolysis, which make it possible to use PPy as a carbon resource and template for the synthesis of N-doped CNFs, as shown in Fig. 13. The synthesized N-doped porous CNF network could serve not only as an adsorbent for CO_2 capture, but also as a catalyst for CO_2 conversion. In addition, it was found that a few factors, such as KOH activation and activation temperature, were crucial for obtaining the specific surface area and N content. For instance, a large amount of KOH and a high activation temperature were beneficial to the formation of a porous structure and high specific surface area, but would result in low N content. Therefore, the optimal experimental conditions should be adjusted to achieve the best overall performance.

Ma *et al.* prepared porous CNFs from polyvinylidene fluoride (PVDF)–polyvinyl pyrrolidone/PVP core–shell NFs, which have excellent capacitance and a high carbon dioxide adsorption rate.[124] In a similar study, Iqbal and co-workers demonstrated the synthesis of nicotinic acid salt/CNT-doped CNFs for high performance energy storage and CO_2 adsorption.[125] The development of these hybrid materials provides a facile way to achieve various multifunctional applications.

In a very recent study, Zainab *et al.* mixed PVP and PAN solution together for electrospinning to form PNFs, which were then dried in a vacuum and hydrolyzed to obtain porous CNFs after selectively removing the PVP precursor.[126] This created material has good selectivity for CO_2 and could be useful for the further fabrication of 3D CNF-based functional nanomaterials for the capture of CO_2.

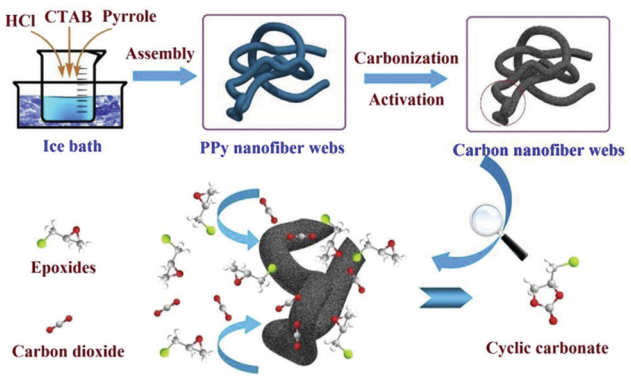

Fig. 13 A schematic illustration of the synthetic route to porous CNF networks for application in CO_2 capture. Reprinted images with permission from ref. 123. Copyright 2016, Elsevier BV.

4.3. Shielding against electromagnetic radiation pollution

With the fast development of electronic devices, both electronic and electromagnetic devices, such as household appliances, wireless communication systems, and lighting equipment, have caused electromagnetic radiation pollution, which affects human lives and health. It has been found that metal materials, magnetic materials, and polymer materials could be used to produce an electrostatic shielding effect under certain conditions when they are combined with conductive fillers.[127,128] On the other hand, it is possible to use materials to result in microwave absorption, in which the electromagnetic radiation is transformed into other forms of motion through physical action, and then into heat energy through the dissipation of motion.[129,130]

CNFs have been widely used for electromagnetic radiation and microwave shielding due to their high aspect ratio, low preparation cost, and excellent mechanical and electrical properties.[131,132] They can be used not only in the preparation of electrostatic shielding materials, but also in microwave absorption by structural adjustment or doping with other materials.[133] In addition, this is a universal and effective way to combine carbon materials with metal oxides, metals, and other magnetic materials to improve the microwave absorption performance of carbon materials. The 3D network structure is conducive to the dissipation of micro currents and the generation of heat energy, resulting in high dielectric loss and improving the microwave absorption effect. Therefore, 3D CNFs and their composites have more advantages in this field.[128]

For example, Wang *et al.* reported that a 3D conductive network structure composed of 1D CNFs can obtain a high effective absorption bandwidth, which could be utilized to synthesize a lightweight 3D FeCo/CNF composite for microwave absorption.[133] Compared to pure metals, ferromagnetic metal/alloy materials based on Fe, Co, and Ni have larger complex permeability, broader resonance frequency, and higher magnetic loss due to their unique structure and properties, which are beneficial for the absorption of microwaves in the GHz range. Zhang and co-workers studied and evaluated the microwave absorption performance of tubular CNFs (TCNFs), and the corresponding microwave weakening mechanism was studied in detail.[128] As shown in Fig. 14, TCNFs could form a 3D conductive network in the matrix, in which the electrons in the network attenuated microwaves into the form of microcurrents. In addition, electromagnetic waves were reflected and scattered on the surface of and inside the formed 3D materials. Meanwhile, the high specific surface area of the materials provided more interfaces, which could enhance the interfacial polarization and Debye relaxation ability. Furthermore, the abundant pores and channels were important in improving the characteristic impedance matching of the materials and increasing the microwave absorbing ability of CNF-based materials.

In another case, Luo and co-workers reported that a kind of 3D CNFs prepared by the pyrolysis of bacterial cellulose could

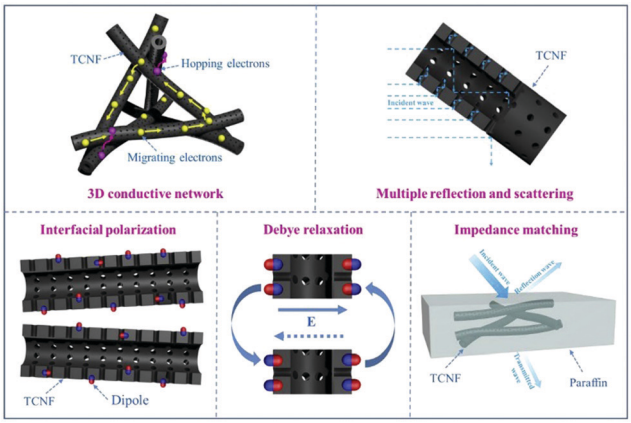

Fig. 14 A schematic diagram of the microwave adsorption mechanism in tubular CNFs. Reprinted with permission from ref. 128. Copyright 2019, Elsevier BV.

be used as the substrate to conjugate with highly dispersed Fe_3O_4 NPs for improved microwave absorption performance.[134]

5. Conclusions and perspectives

In summary, we have briefly introduced the synthesis of CNFs and fabrication strategies for various 3D CNFs and CNF-based composites. Their interconnected structure, large porosity, and high specific surface area make them very efficient in the process of mass transfer and provide more active sites. CNFs with a 3D structure have been widely used in energy storage and environmental science due to their unique properties and functions. To improve catalytic activity and adsorption ability, the doping of CNFs with heteroatoms, metal NPs, transition metallic NPs, and other nanoscale building blocks has been explored. The fabrication of CNF-based nanomaterials with novel structures and functions has been the main aim in this research field.

Here we would like to discuss potential studies that could be performed for energy and environmental applications in the future. First, there have been a lot of studies on the doping of CNFs with various nanomaterials with improved performance for electrode materials and adsorption materials; however, the relationships between the structural tailoring or modification of CNFs and their real functions should be investigated in depth *via* other techniques, such as computer simulations, which will be helpful for understanding the doping-induced enhancement mechanism and promoting the design of novel 3D nanomaterials. Second, it is possible to combine 3D CNFs with light-sensitive materials, such as quantum dots, TiO_2, *etc.*, to explore the photochemical and photoelectronic applications of 3D CNF-based nanomaterials: for instance, solar cells, photo-mediated deionization to obtain clean drinking water from seawater, and the photocatalytic degradation of organic dyes in wastewater systems. Third, the use of 3D CNF nanomaterials for energy and environmental applications involves a key challenge: how can the materials be applied for practical applications? Some factors, such as cost, resource availability, performance, stability, and reproducibility, should be considered. In this case, more attention should be focused on the utilization of various biomass materials, including cellulose, chitosan, chitin, and other abundant and cheap materials.

Conflicts of interest

There are no conflicts to declare.

Acknowledgements

The authors are thankful for financial support from the National Natural Science Foundation of China (No. 51873225), the High-Grade Talents Plan of Qingdao University, and the Taishan Scholars Program of Shandong Province (No. tsqn201909104).

Notes and references

1 S. C. Smith and D. F. Rodrigues, Carbon-based nanomaterials for removal of chemical and biological contaminants from water: A review of mechanisms and applications, *Carbon*, 2015, **91**, 122–143.
2 C. Yang, M. E. Denno, P. Pyakurel and B. J. Venton, Recent trends in carbon nanomaterial-based electrochemical sensors for biomolecules: A review, *Anal. Chim. Acta*, 2015, **887**, 17–37.
3 Q. L. Yan, M. Gozin, F. Q. Zhao, A. Cohen and S. P. Pang, Highly energetic compositions based on functionalized carbon nanomaterials, *Nanoscale*, 2016, **8**, 4799–4851.
4 J. Wen, Y. Q. Xu, H. J. Li, A. P. Lu and S. G. Sun, Recent applications of carbon nanomaterials in fluorescence biosensing and bioimaging, *Chem. Commun.*, 2015, **51**, 11346–11358.
5 Y. Li, M. F. Zhang, X. P. Zhang, G. C. Xie, Z. Q. Su and G. Wei, Nanoporous carbon nanofibers decorated with platinum nanoparticles for non-enzymatic electrochemical sensing of h2o2, *Nanomaterials*, 2015, **5**, 1891–1905.
6 Z. Q. Wang, S. S. Wu, J. Wang, A. L. Yu and G. Wei, Carbon nanofiber-based functional nanomaterials for sensor applications, *Nanomaterials*, 2019, **9**, 1045.
7 X. X. Zhou, Y. Wang, C. C. Gong, B. Liu and G. Wei, Production, structural design, functional control, and broad applications of carbon nanofiber-based nanomaterials: A comprehensive review, *Chem. Eng. J.*, 2020, **402**, 126189.
8 C. Alegre, E. Modica, A. Di Blasi, O. Di Blasi, C. Busacca and M. Ferraro, *et al.*, Nico-loaded carbon nanofibers obtained by electrospinning: Bifunctional behavior as air electrodes, *Renewable Energy*, 2018, **125**, 250–259.
9 Y. Zhai, X. Bai, H. N. Cui, J. Y. Zhu, W. Liu and T. X. Zhang, *et al.*, Carbon dot/polyvinylpyrrolidone hybrid nanofibers with efficient solid-state photoluminescence constructed using an electrospinning technique, *Nanotechnology*, 2018, **29**, 2.
10 C. L. Ringor, C. S. Pascua, J. C. B. Villanueva, A. K. H. Garcia, I. J. A. Agulo and Y. Matsushita, *et al.*, Multiwalled

carbon nanofibers and nanocapsules synthesized from plant oil via atmospheric cvd process, *J. Nanosci. Nanotechnol.*, 2017, **17**, 3543–3550.

11 Y. F. Liu, J. J. Luo, C. Helleu, M. Behr, H. Ba and T. Romero, *et al.*, Hierarchical porous carbon fibers/carbon nanofibers monolith from electrospinning/cvd processes as a high effective surface area support platform, *J. Mater. Chem. A*, 2017, **5**, 2151–2162.

12 W. Fang, S. Yang, X. L. Wang, T. Q. Yuan and R. C. Sun, Manufacture and application of lignin-based carbon fibers (lcfs) and lignin-based carbon nanofibers (lcnfs), *Green Chem.*, 2017, **19**, 1794–1827.

13 Y. J. Huang, T. Zhou, S. He, H. Xiao, H. M. Dai and B. H. Yuan, *et al.*, Flame-retardant polyvinyl alcohol/cellulose nanofibers hybrid carbon aerogel by freeze drying with ultra-low phosphorus, *Appl. Surf. Sci.*, 2019, **497**, 143775.

14 H. Gaminian, M. Montazer, A. Bahi, M. Karaaslan and F. Ko, Capacitance performance boost of cellulose-derived carbon nanofibers via carbon and silver nanoparticles, *Cellulose*, 2019, **26**, 2499–2512.

15 D. Pan, M. Ombaba, Z. Y. Zhou, Y. Liu, S. W. Chen and J. Lu, Direct growth of carbon nanofibers to generate a 3d porous platform on a metal contact to enable an oxygen reduction reaction, *ACS Nano*, 2012, **6**, 10720–10726.

16 Q. Shi, Y. D. Wang, Z. M. Wang, Y. P. Lei, B. Wang and N. Wu, *et al.*, Three-dimensional (3d) interconnected networks fabricated via in-situ growth of n-doped graphene/carbon nanotubes on co-containing carbon nanofibers for enhanced oxygen reduction, *Nano Res.*, 2016, **9**, 317–328.

17 Y. P. Zhu, Y. Jing, A. Vasileff, T. Heine and S. Z. Qiao, 3d synergistically active carbon nanofibers for improved oxygen evolution, *Adv. Energy Mater.*, 2017, **7**, 1602928.

18 Z. Y. Wu, H. W. Liang, L. F. Chen, B. C. Hu and S. H. Yu, Bacterial cellulose: A robust platform for design of three dimensional carbon-based functional nanomaterials, *Acc. Chem. Res.*, 2016, **49**, 96–105.

19 W. C. Wan, Y. H. Lin, A. Prakash and Y. Zhou, Three-dimensional carbon-based architectures for oil remediation: From synthesis and modification to functionalization, *J. Mater. Chem. A*, 2016, **4**, 18687–18705.

20 L. F. Zhang, A. Aboagye, A. Kelkar, C. L. Lai and H. Fong, A review: Carbon nanofibers from electrospun polyacrylonitrile and their applications, *J. Mater. Sci.*, 2014, **49**, 463–480.

21 L. C. Feng, N. Xie and J. Zhong, Carbon nanofibers and their composites: A review of synthesizing, properties and applications, *Materials*, 2014, **7**, 3919–3945.

22 S. J. Peng, L. L. Li, J. K. Y. Lee, L. L. Tian, M. Srinivasan and S. Adams, *et al.*, Electrospun carbon nanofibers and their hybrid composites as advanced materials for energy conversion and storage, *Nano Energy*, 2016, **22**, 361–395.

23 B. A. Zhang, F. Y. Kang, J. M. Tarascon and J. K. Kim, Recent advances in electrospun carbon nanofibers and their application in electrochemical energy storage, *Prog. Mater. Sci.*, 2016, **76**, 319–380.

24 Z. Q. Su, J. W. Ding and G. Wei, Electrospinning: A facile technique for fabricating polymeric nanofibers doped with carbon nanotubes and metallic nanoparticles for sensor applications, *RSC Adv.*, 2014, **4**, 52598–52610.

25 L. Tao, Y. B. Huang, X. Q. Yang, Y. W. Zheng, C. Liu and M. W. Di, *et al.*, Flexible anode materials for lithium-ion batteries derived from waste biomass-based carbon nanofibers: I. Effect of carbonization temperature, *RSC Adv.*, 2018, **8**, 7102–7109.

26 X. Lu, P. Wang, K. Liu, C. M. Niu and H. K. Wang, Encapsulating nanoparticulate sb/moox into porous carbon nanofibers via electrospinning for efficient lithium storage, *Chem. Eng. J.*, 2018, **336**, 701–709.

27 F. Wu, R. Q. Dong, Y. Bai, Y. Li, G. H. Chen and Z. H. Wang, *et al.*, Phosphorus-doped hard carbon nanofibers prepared by electrospinning as an anode in sodium-ion batteries, *ACS Appl. Mater. Interfaces*, 2018, **10**, 21335–21342.

28 W. M. Chen, S. Chen, Y. Morsi, H. El-Hamshary, M. El-Newehy and C. Y. Fan, *et al.*, Superabsorbent 3d scaffold based on electrospun nanofibers for cartilage tissue engineering, *ACS Appl. Mater. Interfaces*, 2016, **8**, 24415–24425.

29 J. Y. Xu, X. Liu, X. Y. Ren and G. H. Gao, The role of chemical and physical crosslinking in different deformation stages of hybrid hydrogels, *Eur. Polym. J.*, 2018, **100**, 86–95.

30 N. Wang, Y. S. Si, N. Wang, G. Sun, M. El-Newehy and S. S. Al-Deyab, *et al.*, Multilevel structured polyacrylonitrile/silica nanofibrous membranes for high-performance air filtration, *Sep. Purif. Technol.*, 2014, **126**, 44–51.

31 L. H. Leung, S. Fan and H. E. Naguib, Fabrication of 3d electrospun structures from poly(lactide-*co*-glycolide acid)-nano-hydroxyapatite composites, *J. Polym. Sci., Part B: Polym. Phys.*, 2012, **50**, 242–249.

32 T. Xu, Z. P. Liang, B. Ding, Q. Feng and H. Fong, Polymer blend nanofibers containing polycaprolactone as biocompatible and biodegradable binding agent to fabricate electrospun three-dimensional scaffolds/structures, *Polymer*, 2018, **151**, 299–306.

33 S. S. Yao, R. D. Guo, F. W. Xie, Z. Z. Wu, K. D. Gao and C. J. Zhang, *et al.*, Electrospun three-dimensional cobalt decorated nitrogen doped carbon nanofibers network as freestanding electrode for lithium/sulfur batteries, *Electrochim. Acta*, 2020, **337**, 135765.

34 S. Matsuda, The effect of electrical conductivity on lithium metal deposition in 3d carbon nanofiber matrices, *Carbon*, 2019, **154**, 370–374.

35 L. J. Zhang, G. L. Xia, Z. P. Guo, D. L. Sun, X. G. Li and X. B. Yu, In situ fabrication of three-dimensional nitrogen and boron co-doped porous carbon nanofibers for high performance lithium-ion batteries, *J. Power Sources*, 2016, **324**, 294–301.

36 H. Cheng, Z. Y. Zhou, Y. Q. Li, W. Y. Huang, J. Feng and T. F. Tang, *et al.*, Electrochemiluminescence sensor based on electrospun three-dimensional carbon nanofibers for the detection of difenidol hydrochloride, *Sensors*, 2019, **19**, 3315.

37 A. P. Tiwari, S. H. Chae, G. P. Ojha, B. Dahal, T. Mukhiya and M. Lee, *et al.*, Three-dimensional porous carbonaceous

network with in-situ entrapped metallic cobalt for supercapacitor application, *J. Colloid Interface Sci.*, 2019, **553**, 622–630.

38 R. J. Cui, D. Xu, X. H. Xie, Y. Y. Yi, Y. Quan and M. X. Zhou, *et al.*, Phosphorus-doped helical carbon nanofibers as enhanced sensing platform for electrochemical detection of carbendazim, *Food Chem.*, 2017, **221**, 457–463.

39 H. A. Duan, J. Y. Liang and Z. H. Xia, Synthetic hierarchical nanostructures: Growth of carbon nanofibers on microfibers by chemical vapor deposition, *Mater. Sci. Eng., B*, 2010, **166**, 190–195.

40 J. Kang, D. H. Shin, K. N. Yun, F. A. Masud, C. J. Lee and M. J. Kim, Super growth of vertically-aligned carbon nanofibers and their field emission properties, *Carbon*, 2014, **79**, 149–155.

41 S. Mishra, H. Nguyen, P. K. Adusei, Y. Y. Hsieh and V. Shanov, Plasma enhanced synthesis of n doped vertically aligned carbon nanofibers on 3d graphene, *Surf. Interface Anal.*, 2019, **51**, 290–297.

42 S. A. Klankowski, G. P. Pandey, B. A. Cruden, J. W. Liu, J. Wu and R. A. Rojeski, *et al.*, Anomalous capacity increase at high-rates in lithium-ion battery anodes based on silicon-coated vertically aligned carbon nanofibers, *J. Power Sources*, 2015, **276**, 73–79.

43 K. Kaneko, R. Nagayama, K. Inoke, W. J. Moon, Z. Horita and Y. Hayashi, *et al.*, Formation of wedge-shaped carbon film by chemical vapor deposition method and observation using transmission electron microscopy, *Scr. Mater.*, 2005, **52**, 1205–1209.

44 J. H. Lee and S. J. Park, Recent advances in preparations and applications of carbon aerogels: A review, *Carbon*, 2020, **163**, 1–18.

45 G. Zhu, H. Y. Wang, H. F. Xu and L. Zhang, Enhanced capacitive deionization by nitrogen-doped porous carbon nanofiber aerogel derived from bacterial-cellulose, *J. Electroanal. Chem.*, 2018, **822**, 81–88.

46 H. Chen, T. Liu, J. R. Mau, W. J. Zhang, Z. J. Jiang and J. Liu, *et al.*, Free-standing n-self-doped carbon nanofiber aerogels for high-performance all-solid-state supercapacitors, *Nano Energy*, 2019, **63**, 103836.

47 L. F. Chen, Y. Feng, H. W. Liang, Z. Y. Wu and S. H. Yu, Macroscopic-scale three-dimensional carbon nanofiber architectures for electrochemical energy storage devices, *Adv. Energy Mater.*, 2017, **7**, 1700826.

48 H. W. Liang, Q. F. Guan, L. F. Chen, Z. Zhu, W. J. Zhang and S. H. Yu, Macroscopic-scale template synthesis of robust carbonaceous nanofiber hydrogels and aerogels and their applications, *Angew. Chem., Int. Ed.*, 2012, **51**, 5101–5105.

49 K. Zhang, F. Y. Xiong, J. P. Zhou, L. Q. Mai and L. N. Zhang, Universal construction of ultrafine metal oxides coupled in n-enriched 3d carbon nanofibers for high-performance lithium/sodium storage, *Nano Energy*, 2020, **67**, 104222.

50 H. Nosrati, R. S. Mamoory, F. Dabir, M. C. Perez, M. A. Rodriguez and D. Q. S. Le, *et al.*, In situ synthesis of three dimensional graphene-hydroxyapatite nano powders via hydrothermal process, *Mater. Chem. Phys.*, 2019, **222**, 251–255.

51 Y. Y. Liu, K. B. Chen, H. Chen, Y. H. Wu, X. Y. Ye and X. Bi, *et al.*, One-step hydrothermal fabrication of three dimensional anatase hierarchical hyacinth-like tio2 arrays for dye-sensitized solar cells, *Thin Solid Films*, 2019, **683**, 42–48.

52 B. K. Kang, Y. H. Song, W. K. Park, S. H. Kwag, B. S. Lim and S. Bin-Kwon, *et al.*, Synthesis and characterization of a mesoporous and three dimensional n-doped graphene structure *via* the couette-taylor flow and hydrothermal method, *J. Eur. Ceram. Soc.*, 2017, **37**, 3673–3680.

53 T. L. Zhao, X. Y. Gao, Z. J. Wei, K. J. Guo, F. Wu and L. Li, *et al.*, Three-dimensional li1.2ni0.2mn0.6o2 cathode materials synthesized by a novel hydrothermal method for lithium-ion batteries, *J. Alloys Compd.*, 2018, **757**, 16–23.

54 S. Feng, J. H. Song, S. F. Fu, C. Z. Zhu, Q. R. Shi and M. K. Song, *et al.*, One-step synthesis of carbon nanosheet-decorated carbon nanofibers as a 3d interconnected porous carbon scaffold for lithium-sulfur batteries, *J. Mater. Chem. A*, 2017, **5**, 23737–23743.

55 J. G. Ju, L. T. Zhang, H. S. Shi, Z. J. Li, W. M. Kang and B. W. Cheng, Three-dimensional porous carbon nanofiber loading mos2 nanoflake-flowerballs as a high-performance anode material for li-ion capacitor, *Appl. Surf. Sci.*, 2019, **484**, 392–402.

56 K. T. Alali, J. Y. Liu, K. Aljebawi, Q. Liu, R. R. Chen and J. Yu, *et al.*, 3d hybrid ni-multiwall carbon nanotubes/carbon nanofibers for detecting sarin nerve agent at room temperature, *J. Alloys Compd.*, 2019, **780**, 680–689.

57 F. Lu, J. G. Wang, X. L. Sun and Z. J. Chang, 3d hierarchical carbon nanofibers/tio2@mos2 core-shell heterostructures by electrospinning, hydrothermal and in-situ growth for flexible electrode materials, *Mater. Des.*, 2020, **189**, 108503.

58 B. Dahal, T. Mukhiya, G. P. Ojha, A. Muthurasu, S. H. Chae and T. Kim, *et al.*, In-built fabrication of mof assimilated b/n co-doped 3d porous carbon nanofiber network as a binder-free electrode for supercapacitors, *Electrochim. Acta*, 2019, **301**, 209–219.

59 C. X. Lv, H. L. Liu, D. H. Li, S. Chen, H. W. Zhang and X. L. She, *et al.*, Ultrafine fese nanoparticles embedded into 3d carbon nanofiber aerogels with fese/carbon interface for efficient and long-life sodium storage, *Carbon*, 2019, **143**, 106–115.

60 W. Lei, H. J. Zhang, D. Z. Liu and L. X. Lin, Fabrication of nitrogen and sulfur co-doped carbon nanofibers with three-dimensional architecture for high performance supercapacitors, *Appl. Surf. Sci.*, 2019, **495**, 143572.

61 L. F. Chen, Z. H. Huang, H. W. Liang, H. L. Gao and S. H. Yu, Three-dimensional heteroatom-doped carbon nanofiber networks derived from bacterial cellulose for supercapacitors, *Adv. Funct. Mater.*, 2014, **24**, 5104–5111.

62 F. L. Lai, Y. P. Huang, L. Z. Zuo, H. H. Gu, Y. E. Miao and T. X. Liu, Electrospun nanofiber-supported carbon aerogel as a versatile platform toward asymmetric supercapacitors, *J. Mater. Chem. A*, 2016, **4**, 15861–15869.

63 X. F. Zhang, J. Q. Zhao, X. He, Q. Y. Li, C. H. Ao and T. Xia, *et al.*, Mechanically robust and highly compressible electrochemical supercapacitors from nitrogen-doped carbon aerogels, *Carbon*, 2018, **127**, 236–244.

64 M. Zhang, D. Z. Yang, S. Y. Zhang, T. Xu, Y. Z. Shi and Y. X. Liu, *et al.*, Elastic and hierarchical carbon nanofiber aerogels and their hybrids with carbon nanotubes and cobalt oxide nanoparticles for high-performance asymmetric supercapacitors, *Carbon*, 2020, **158**, 873–884.

65 C. H. Lin, C. H. Tsai, F. G. Tseng, I. C. Chen and C. K. Hsieh, Electrochemical pulse deposition of ni nanoparticles on the 3d graphene network to synthesize vertical cnfs as the full-carbon hybrid nanoarchitecture for supercapacitors, *Mater. Lett.*, 2017, **192**, 40–43.

66 Y. C. Qiu, G. Z. Li, Y. Hou, Z. H. Pan, H. F. Li and W. F. Li, *et al.*, Vertically aligned carbon nanotubes on carbon nanofibers: A hierarchical three-dimensional carbon nanostructure for high-energy flexible supercapacitors, *Chem. Mater.*, 2015, **27**, 1194–1200.

67 H. Y. Zhang, Y. T. Dai, H. Zhang, W. Wang, Q. Y. Huang and Y. L. Chen, *et al.*, Synthesis and electrochemical measurement of three dimensional carbon nanofibers/co3o4-polyaniline composites as supercapacitor electrode materials in neutral electrolyte, *Int. J. Electrochem. Sci.*, 2016, **11**, 6279–6286.

68 F. L. Lai, Y. P. Huang, Y. E. Miao and T. X. Liu, Controllable preparation of multi-dimensional hybrid materials of nickel-cobalt layered double hydroxide nanorods/nanosheets on electrospun carbon nanofibers for high-performance supercapacitors, *Electrochim. Acta*, 2015, **174**, 456–463.

69 Z. K. Ghouri, N. A. M. Barakat, M. Obaid, J. H. Lee and H. Y. Kim, Co/ceo2-decorated carbon nanofibers as effective non-precious electro-catalyst for fuel cells application in alkaline medium, *Ceram. Int.*, 2015, **41**, 2271–2278.

70 M. A. Alvi and M. S. Akhtar, An effective and low cost pd-ce bimetallic decorated carbon nanofibers as electro-catalyst for direct methanol fuel cells applications, *J. Alloys Compd.*, 2016, **684**, 524–529.

71 G. Massaglia, V. Margaria, A. Sacco, M. Castellino, A. Chiodoni and F. C. Pirri, *et al.*, N-doped carbon nanofibers as catalyst layer at cathode in single chamber microbial fuel cells, *Int. J. Hydrogen Energy*, 2019, **44**, 4442–4449.

72 X. Tang, Z. Y. Xie, Q. Z. Huang, G. F. Chen, M. Hou and B. L. Yi, Mass-transport-controlled, large-area, uniform deposition of carbon nanofibers and their application in gas diffusion layers of fuel cells, *Nanoscale*, 2015, **7**, 7971–7979.

73 X. B. Cheng, Q. Zhang, H. F. Wang, G. L. Tian, J. Q. Huang and H. J. Peng, *et al.*, Nitrogen-doped herringbone carbon nanofibers with large lattice spacings and abundant edges: Catalytic growth and their applications in lithium ion batteries and oxygen reduction reactions, *Catal. Today*, 2015, **249**, 244–251.

74 Y. L. Cheng, L. Huang, X. Xiao, B. Yao, L. Y. Yuan and T. Q. Li, *et al.*, Flexible and cross-linked n-doped carbon nanofiber network for high performance freestanding supercapacitor electrode, *Nano Energy*, 2015, **15**, 66–74.

75 S. L. Chen, H. Q. Hou, F. Harnisch, S. A. Patil, A. A. Carmona-Martinez and S. Agarwal, *et al.*, Electrospun and solution blown three-dimensional carbon fiber nonwovens for application as electrodes in microbial fuel cells, *Energy Environ. Sci.*, 2011, **4**, 1417–1421.

76 P. Khare, J. Ramkumar and N. Verma, Carbon nanofiber-skinned three dimensional ni/carbon micropillars: High performance electrodes of a microbial fuel cell, *Electrochim. Acta*, 2016, **219**, 88–98.

77 Q. Shi, Y. P. Lei, Y. D. Wang, H. P. Wang, L. H. Jiang and H. L. Yuan, *et al.*, B, n-codoped 3d micro-/mesoporous carbon nanofibers web as efficient metal-free catalysts for oxygen reduction, *Curr. Appl. Phys.*, 2015, **15**, 1606–1614.

78 X. Song, S. Q. Wang, Y. Bao, G. X. Liu, W. P. Sun and L. X. Ding, *et al.*, A high strength, free-standing cathode constructed by regulating graphitization and the pore structure in nitrogen-doped carbon nanofibers for flexible lithium-sulfur batteries, *J. Mater. Chem. A*, 2017, **5**, 6832–6839.

79 Y. X. Liu, L. Si, Y. C. Du, X. S. Zhou, Z. H. Dai and J. C. Bao, Strongly bonded selenium/microporous carbon nanofibers composite as a high-performance cathode for lithium-selenium batteries, *J. Phys. Chem. C*, 2015, **119**, 27316–27321.

80 G. H. An, D. Y. Lee and H. J. Ahn, Tunneled mesoporous carbon nanofibers with embedded zno nanoparticles for ultrafast lithium storage, *ACS Appl. Mater. Interfaces*, 2017, **9**, 12478–12485.

81 Y. Liu, J. S. Chen, Z. K. Liu, H. Y. Xu, Y. H. Zheng and J. S. Zhong, *et al.*, Facile fabrication of fe3o4 nanoparticle/carbon nanofiber aerogel from fe-ion cross-linked cellulose nanofibrils as anode for lithium-ion battery with superhigh capacity, *J. Alloys Compd.*, 2020, **829**, 154541.

82 C. Q. Shang, L. J. Cao, M. Y. Yang, Z. Y. Wang, M. C. Li and G. F. Zhou, *et al.*, Freestanding mo2c-decorating n-doped carbon nanofibers as 3d current collector for ultra-stable li-s batteries, *Energy Storage Mater.*, 2019, **18**, 375–381.

83 J. D. Zhu, C. Chen, Y. Lu, Y. Q. Ge, H. Jiang and K. Fu, *et al.*, Nitrogen-doped carbon nanofibers derived from polyacrylonitrile for use as anode material in sodium-ion batteries, *Carbon*, 2015, **94**, 189–195.

84 Y. C. Liu, N. Zhang, L. F. Jiao and J. Chen, Tin nanodots encapsulated in porous nitrogen-doped carbon nanofibers as a free-standing anode for advanced sodium-ion batteries, *Adv. Mater.*, 2015, **27**, 6702–6707.

85 D. T. Ma, Y. L. Li, H. W. Mi, S. Luo, P. X. Zhang and Z. Q. Lin, *et al.*, Robust sno2-x nanoparticle-impregnated carbon nanofibers with outstanding electrochemical performance for advanced sodium-ion batteries, *Angew. Chem., Int. Ed.*, 2018, **57**, 8901–8905.

86 M. Wang, Y. Yang, Z. Z. Yang, L. Gu, Q. W. Chen and Y. Yu, Sodium-ion batteries: Improving the rate capability of 3d interconnected carbon nanofibers thin film by boron, nitrogen dual-doping, *Adv. Sci.*, 2017, **4**, 1600468.

87 H. Yin, H. Q. Qu, Z. T. Liu, R. Z. Jiang, C. Li and M. Q. Zhu, Long cycle life and high rate capability of three

dimensional cose2 grain-attached carbon nanofibers for flexible sodium-ion batteries, *Nano Energy*, 2019, **58**, 715–723.

88 H. L. Liu, C. X. Lv, S. Chen, X. Y. Song, B. H. Liu and J. Sun, *et al.*, Fe-alginate biomass-derived fes/3d interconnected carbon nanofiber aerogels as anodes for high performance sodium-ion batteries, *J. Alloys Compd.*, 2019, **795**, 54–59.

89 R. A. Adams, J. M. Syu, Y. P. Zhao, C. T. Lo, A. Varma and V. G. Pol, Binder-free n- and o-rich carbon nanofiber anodes for long cycle life k-ion batteries, *ACS Appl. Mater. Interfaces*, 2017, **9**, 17872–17881.

90 Z. Huang, Z. Chen, S. S. Ding, C. M. Chen and M. Zhang, Enhanced conductivity and properties of sno2-graphene-carbon nanofibers for potassium-ion batteries by graphene modification, *Mater. Lett.*, 2018, **219**, 19–22.

91 S. K. Zhang, Z. G. Xu, H. H. Duan, A. D. Xu, Q. Xia and Y. R. Yan, *et al.*, N-doped carbon nanofibers with internal cross-linked multiple pores for both ultra-long cycling life and high capacity in highly durable k-ion battery anodes, *Electrochim. Acta*, 2020, **337**, 135767.

92 K. Han, Z. W. Liu, P. Li, Q. Y. Yu, W. Wang and C. Y. Lao, *et al.*, High-throughput fabrication of 3d n-doped graphenic framework coupled with fe3c@porous graphite carbon for ultrastable potassium ion storage, *Energy Storage Mater.*, 2019, **22**, 185–193.

93 J. C. Du, S. S. Gao, P. H. Shi, J. C. Fan, Q. J. Xu and Y. L. Min, Three-dimensional carbonaceous for potassium ion batteries anode to boost rate and cycle life performance, *J. Power Sources*, 2020, **451**, 227727.

94 B. J. Yang, J. T. Chen, L. Y. Liu, P. J. Ma, B. Liu and J. W. Lang, *et al.*, 3d nitrogen-doped framework carbon for high-performance potassium ion hybrid capacitor, *Energy Storage Mater.*, 2019, **23**, 522–529.

95 S. Bao, S. H. Luo, S. X. Yan, Z. Y. Wang, Q. Wang and J. Feng, *et al.*, Nano-sized moo2 spheres interspersed three-dimensional porous carbon composite as advanced anode for reversible sodium/potassium ion storage, *Electrochim. Acta*, 2019, **307**, 293–301.

96 Z. Y. Wang, K. Z. Dong, D. Wang, S. H. Luo, Y. G. Liu and Q. Wang, *et al.*, Ultrafine sno2 nanoparticles encapsulated in 3d porous carbon as a, high-performance anode material for potassium-ion batteries, *J. Power Sources*, 2019, **441**, 227191.

97 W. M. Zhang, J. T. Chen, Y. Q. Liu, S. M. Liu, X. T. Li and K. Yang, *et al.*, Decoration of hollow nitrogen-doped carbon nanofibers with tapered rod-shaped nico2s4 as a 3d structural high-rate and long-lifespan self-supported anode material for potassium-ion batteries, *J. Alloys Compd.*, 2020, **823**, 153631.

98 T. T. Yang, H. Zhu, M. Wan, L. Dong, M. Zhang and M. L. Du, Highly efficient and durable ptco alloy nanoparticles encapsulated in carbon nanofibers for electrochemical hydrogen generation, *Chem. Commun.*, 2016, **52**, 990–993.

99 J. D. Chen, D. N. Yu, W. S. Liao, M. D. Zheng, L. F. Xiao and H. Zhu, *et al.*, Wo3-x nanoplates grown on carbon nanofibers for an efficient electrocatalytic hydrogen evolution reaction, *ACS Appl. Mater. Interfaces*, 2016, **8**, 18132–18139.

100 K. H. Chung, S. Jeong, B. J. Kim, K. H. An, Y. K. Park and S. C. Jung, Enhancement of photocatalytic hydrogen production by liquid phase plasma irradiation on metal-loaded tio2/carbon nanofiber photocatalysts, *Int. J. Hydrogen Energy*, 2018, **43**, 11422–11429.

101 J. C. Xu, J. Rong, F. X. Qiu, Y. Zhu, K. L. Mao and Y. Y. Fang, *et al.*, Highly dispersive nico2s4 nanoparticles anchored on nitrogen-doped carbon nanofibers for efficient hydrogen evolution reaction, *J. Colloid Interface Sci.*, 2019, **555**, 294–303.

102 J. L. Zhang, W. Jia, S. Q. Dang and Y. L. Cao, Sub-5 nm octahedral platinum-copper nanostructures anchored on nitrogen-doped porous carbon nanofibers for remarkable electrocatalytic hydrogen evolution, *J. Colloid Interface Sci.*, 2020, **560**, 161–168.

103 H. H. Gu, Y. P. Huang, L. Z. Zuo, W. Fan and T. X. Liu, Graphene sheets wrapped carbon nanofibers as a highly conductive three-dimensional framework for perpendicularly anchoring of mos2: Advanced electrocatalysts for hydrogen evolution reaction, *Electrochim. Acta*, 2016, **219**, 604–613.

104 Y. Mi, L. Y. Wen, Z. J. Wang, D. W. Cao, H. P. Zhao and Y. L. Zhou, *et al.*, Ultra-low mass loading of platinum nanoparticles on bacterial cellulose derived carbon nanofibers for efficient hydrogen evolution, *Catal. Today*, 2016, **262**, 141–145.

105 G. L. Cao, Y. M. Yan, T. Liu, D. Rooney, Y. F. Guo and K. N. Sun, Three-dimensional porous carbon nanofiber networks decorated with cobalt-based nanoparticles: A robust electrocatalyst for efficient water oxidation, *Carbon*, 2015, **94**, 680–686.

106 Y. Li, H. X. Li, K. Z. Cao, T. Jin, X. J. Wang and H. M. Sun, *et al.*, Electrospun three dimensional co/cop@nitrogen-doped carbon nanofibers network for efficient hydrogen evolution, *Energy Storage Mater.*, 2018, **12**, 44–53.

107 W. Q. Zhu, Y. L. Lin, W. W. Kang, H. Y. Quan, Y. Y. Zhang and M. L. Chang, *et al.*, An aerogel adsorbent with bio-inspired interfacial adhesion between graphene and mos2 sheets for water treatment, *Appl. Surf. Sci.*, 2020, **512**, 145717.

108 F. Rouzafzay, R. Shidpour, M. Z. M. Al-Abri, F. Qaderi, A. Ahmadi and M. T. Z. Myint, Graphene@zno nanocompound for short-time water treatment under sun-simulated irradiation: Effect of shear exfoliation of graphene using kitchen blender on photocatalytic degradation, *J. Alloys Compd.*, 2020, **829**, 154614.

109 K. Roy, A. Mukherjee, N. R. Maddela, S. Chakraborty, B. X. Shen and M. Li, *et al.*, Outlook on the bottleneck of carbon nanotube in desalination and membrane-based water treatment-a review, *J. Environ. Chem. Eng.*, 2020, **8**, 103572.

110 X. X. Cheng, W. W. Zhou, P. J. Li, Z. X. Ren, D. J. Wu and C. W. Luo, *et al.*, Improving ultrafiltration membrane performance with pre-deposited carbon nanotubes/nanofibers

layers for drinking water treatment, *Chemosphere*, 2019, **234**, 545–557.

111 B. M. Thamer, A. Aldalbahi, M. Moydeen, A. M. Al-Enizi, H. El-Hamshary and M. Singh, *et al.*, Alkali-activated electrospun carbon nanofibers as an efficient bifunctional adsorbent for cationic and anionic dyes, *Colloids Surf., A*, 2019, **582**, 123835.

112 Z. Youssef, L. Colombeau, N. Yesmurzayeva, F. Baros, R. Vanderesse and T. Hamieh, *et al.*, Dye-sensitized nanoparticles for heterogeneous photocatalysis: Cases studies with tio2, zno, fullerene and graphene for water purification, *Dyes Pigm.*, 2018, **159**, 49–71.

113 F. Gong, W. B. Wang, H. Li, D. Xia, Q. W. Dai and X. L. Wu, *et al.*, Solid waste and graphite derived solar steam generator for highly-efficient and cost-effective water purification, *Appl. Energy*, 2020, **261**, 114410.

114 R. Gusain, N. Kumar and S. S. Ray, Recent advances in carbon nanomaterial-based adsorbents for water purification, *Coord. Chem. Rev.*, 2020, **405**, 213111.

115 N. Baig, F. I. Alghunaimi and T. A. Saleh, Hydrophobic and oleophilic carbon nanofiber impregnated styrofoam for oil and water separation: A green technology, *Chem. Eng. J.*, 2019, **360**, 1613–1622.

116 Y. Shen, L. Li, K. J. Xiao and J. Y. Xi, Constructing three-dimensional hierarchical architectures by integrating carbon nanofibers into graphite felts for water purification, *ACS Sustainable Chem. Eng.*, 2016, **4**, 2351–2358.

117 Y. Liu, J. Q. Ma, T. Lu and L. K. Pan, Electrospun carbon nanofibers reinforced 3d porous carbon polyhedra network derived from metal-organic frameworks for capacitive deionization, *Sci. Rep.*, 2016, **6**, 32784.

118 Y. J. Li, Y. Liu, M. Wang, X. T. Xu, T. Lu and C. Q. Sun, *et al.*, Phosphorus-doped 3d carbon nanofiber aerogels derived from bacterial-cellulose for highly-efficient capacitive deionization, *Carbon*, 2018, **130**, 377–383.

119 H. W. Li, Z. G. Tang, Z. M. He, X. Gui, L. P. Cui and X. Z. Mao, Structure-activity relationship for co2 absorbent, *Energy*, 2020, **197**, 117166.

120 Y. C. Chiang, C. Y. Wu and Y. J. Chen, Effects of activation on the properties of electrospun carbon nanofibers and their adsorption performance for carbon dioxide, *Sep. Purif. Technol.*, 2020, **233**, 116040.

121 N. Ali, A. A. Babar, Y. F. Zhang, N. Iqbal, X. F. Wang and J. Y. Yu, *et al.*, Porous, flexible, and core-shell structured carbon nanofibers hybridized by tin oxide nanoparticles for efficient carbon dioxide capture, *J. Colloid Interface Sci.*, 2020, **560**, 379–387.

122 X. Zong, J. Zhang, J. Q. Zhang, W. Luo, A. Zuttel and Y. P. Xiong, Synergistic cu/ceo2 carbon nanofiber catalysts for efficient co2 electroreduction, *Electrochem. Commun.*, 2020, **114**, 106716.

123 Y. Li, B. Zou, C. W. Hu and M. H. Cao, Nitrogen-doped porous carbon nanofiber webs for efficient co2 capture and conversion, *Carbon*, 2016, **99**, 79–89.

124 S. Ma, Y. X. Wang, Z. Y. Liu, M. N. Huang, H. Yang and Z. L. Xu, Preparation of carbon nanofiber with multilevel gradient porous structure for supercapacitor and co2 adsorption, *Chem. Eng. Sci.*, 2019, **205**, 181–189.

125 N. Iqbal, X. F. Wang, A. A. Babar, J. Y. Yu and B. Ding, Highly flexible nico2o4/cnts doped carbon nanofibers for co2 adsorption and supercapacitor electrodes, *J. Colloid Interface Sci.*, 2016, **476**, 87–93.

126 G. Zainab, A. A. Babar, N. Ali, A. A. Aboalhassan, X. F. Wang and J. Y. Yu, *et al.*, Electrospun carbon nanofibers with multi-aperture/opening porous hierarchical structure for efficient co2 adsorption, *J. Colloid Interface Sci.*, 2020, **561**, 659–667.

127 M. Bayat, H. Yang, F. K. Ko, D. Michelson and A. Mei, Electromagnetic interference shielding effectiveness of hybrid multifunctional fe3o4/carbon nanofiber composite, *Polymer*, 2014, **55**, 936–943.

128 J. Q. Wang, H. Y. Yu, Z. T. Yang, A. B. Zhang, Q. Y. Zhang and B. L. Zhang, Tubular carbon nanofibers: Synthesis, characterization and applications in microwave absorption, *Carbon*, 2019, **152**, 255–266.

129 H. W. Zhen, H. G. Wang and X. L. Xu, Preparation of porous carbon nanofibers with remarkable microwave absorption performance through electrospinning, *Mater. Lett.*, 2019, **249**, 210–213.

130 Y. Li, B. Shen, X. L. Pei, Y. G. Zhang, D. Yi and W. T. Zhai, *et al.*, Ultrathin carbon foams for effective electromagnetic interference shielding, *Carbon*, 2016, **100**, 375–385.

131 X. H. Hong and D. D. L. Chung, Carbon nanofiber mats for electromagnetic interference shielding, *Carbon*, 2017, **111**, 529–537.

132 Y. J. Yan, H. Xia, Y. Q. Fu, Z. Z. Xu and Q. Q. Ni, Carbon nanofiber-structured polyurethane foams for compaction-adjustable microwave shielding, *Mater. Chem. Phys.*, 2020, **246**, 122808.

133 Y. J. Wang, Y. Sun, Y. Zong, T. G. Zhu, L. X. Zhang and X. H. Li, *et al.*, Carbon nanofibers supported by feco nanocrystals as difunctional magnetic/dielectric composites with broadband microwave absorption performance, *J. Alloys Compd.*, 2020, **824**, 153980.

134 H. L. Luo, Y. Zhang, Z. W. Yang, G. Y. Xiong and Y. Z. Wan, Constructing superior carbon-nanofiber-based composite microwave absorbers by engineering dispersion and loading of fe3o4 nanoparticles on three-dimensional carbon nanofibers derived from bacterial cellulose, *Mater. Chem. Phys.*, 2017, **201**, 130–138.